

AD\_\_\_\_\_

AWARD NUMBER: W81XWH-05-1-0476

TITLE: Estrogen Receptor Driven Inhibitor Synthesis

PRINCIPAL INVESTIGATOR: Phani Kumar Pullela, Ph.D.

CONTRACTING ORGANIZATION: Marquette University  
Milwaukee, Wisconsin 53233-2310

REPORT DATE: September 2006

TYPE OF REPORT: Final

PREPARED FOR: U.S. Army Medical Research and Materiel Command  
Fort Detrick, Maryland 21702-5012

DISTRIBUTION STATEMENT: Approved for Public Release;  
Distribution Unlimited

The views, opinions and/or findings contained in this report are those of the author(s) and should not be construed as an official Department of the Army position, policy or decision unless so designated by other documentation.

# REPORT DOCUMENTATION PAGE

*Form Approved*  
*OMB No. 0704-0188*

Public reporting burden for this collection of information is estimated to average 1 hour per response, including the time for reviewing instructions, searching existing data sources, gathering and maintaining the data needed, and completing and reviewing this collection of information. Send comments regarding this burden estimate or any other aspect of this collection of information, including suggestions for reducing this burden to Department of Defense, Washington Headquarters Services, Directorate for Information Operations and Reports (0704-0188), 1215 Jefferson Davis Highway, Suite 1204, Arlington, VA 22202-4302. Respondents should be aware that notwithstanding any other provision of law, no person shall be subject to any penalty for failing to comply with a collection of information if it does not display a currently valid OMB control number. **PLEASE DO NOT RETURN YOUR FORM TO THE ABOVE ADDRESS.**

<b>1. REPORT DATE (DD-MM-YYYY)</b> 01-09-2006		<b>2. REPORT TYPE</b> Final		<b>3. DATES COVERED (From - To)</b> 1 Sep 2005 – 31 Aug 2006	
<b>4. TITLE AND SUBTITLE</b>  Estrogen Receptor Driven Inhibitor Synthesis				<b>5a. CONTRACT NUMBER</b>	
				<b>5b. GRANT NUMBER</b> W81XWH-05-1-0476	
				<b>5c. PROGRAM ELEMENT NUMBER</b>	
<b>6. AUTHOR(S)</b>  Phani Kumar Pullela, Ph.D.  E-Mail: <a href="mailto:pullela77@yahoo.com">pullela77@yahoo.com</a>				<b>5d. PROJECT NUMBER</b>	
				<b>5e. TASK NUMBER</b>	
				<b>5f. WORK UNIT NUMBER</b>	
<b>7. PERFORMING ORGANIZATION NAME(S) AND ADDRESS(ES)</b>  Marquette University Milwaukee, Wisconsin 53233-2310				<b>8. PERFORMING ORGANIZATION REPORT NUMBER</b>	
<b>9. SPONSORING / MONITORING AGENCY NAME(S) AND ADDRESS(ES)</b> U.S. Army Medical Research and Materiel Command Fort Detrick, Maryland 21702-5012				<b>10. SPONSOR/MONITOR'S ACRONYM(S)</b>	
				<b>11. SPONSOR/MONITOR'S REPORT NUMBER(S)</b>	
<b>12. DISTRIBUTION / AVAILABILITY STATEMENT</b> Approved for Public Release; Distribution Unlimited					
<b>13. SUPPLEMENTARY NOTES</b>					
<b>14. ABSTRACT</b>  Purpose: Establish an estrogen receptor (ER) driven inhibitor synthesis procedure and develop a set of building blocks specific for ER-agonist/ER-antagonist interactions. Scope: The ER-binding pocket size is twice the molecular volume of 17-beta-estradiol (E2), giving rise to the tolerance of a diverse class of compounds, resulting in poor interpretability of current SAR models. This project is to establish an ER driven ligand synthesis procedure and define a set of building blocks, which cause specific agonist/antagonist interactions. Major Findings: 1. Estrone was found to react with most of the thiols to give hemi-thioketals as hypothesized in the proposal. 2. An improved synthetic route for the fluorescence polarization reagent (E2-FITC) for assay of ligands against ER was developed. 3. A database of thiols with agonist/antagonist preference for ER was developed using protein-ligand docking. 4. It was concluded that ER is not suitable protein for STD-NMR experiments due to high hydrophobicity and solubility issues. 5. NMR studies on human-ER-LBD may not be practical and use of ER from model systems like zebrafish might address the solubility issues.					
<b>15. SUBJECT TERMS</b> estrogen receptor, ER, agonist, antagonist, enzyme driven inhibitor synthesis, estrone, 17-beta-estradiol, STD-NMR, docking, thiols					
<b>16. SECURITY CLASSIFICATION OF:</b>			<b>17. LIMITATION OF ABSTRACT</b>	<b>18. NUMBER OF PAGES</b>	<b>19a. NAME OF RESPONSIBLE PERSON</b>
<b>a. REPORT</b>	<b>b. ABSTRACT</b>	<b>c. THIS PAGE</b>			<b>USAMRMC</b>
U	U	U	UU	48	<b>19b. TELEPHONE NUMBER (include area code)</b>

## Table of Contents

Cover.....	1
SF 298.....	2
Table of Contents.....	3
Introduction.....	4
Body.....	4
Key Research Accomplishments.....	22
Reportable Outcomes.....	23
Conclusions.....	23
References.....	26
Appendices.....	27

## Introduction

**Subject:** Estrogen receptor driven inhibitor synthesis and development of ER agonist/antagonist database of thiol fragments. **Purpose:** The estrogen receptor (ER)-binding pocket size is twice the molecular volume of 17-beta-estradiol (E2), giving rise to the tolerance of a diverse class of compounds in it, resulting in poor interpretability of current SAR (Structure Activity Relationship) models. Enzyme driven inhibitor synthesis is a recent concept wherein the enzyme itself determines the best inhibitor. This project will establish an ER driven ligand synthesis procedure and define a set of building blocks, which cause specific agonist/antagonist interactions. If successful, this method can be extended to design and synthesize drug molecules in the presence of specific tissues. **Scope of Research:** The E2 analogues are the only reported class of compounds which can act as agonists and antagonists; we propose to react a combinatorial library of thiols with estrone encapsulated by ER. The carbonyl on the D-ring of estrone reacts with appropriate thiols to give an E2 analogue, wherein the driving force for the reaction is a hydrogen bond between the 17-beta-alcohol and His-524. This reaction will be selective for those thiols, which can orient within the binding site to result in agonist interactions similar to E2 (entropy driven). If the attached thiol can push the helix-12 away from the ligand-binding domain to block the TIF-2 binding site, it can produce an antagonist effect similar to ICI 164,384. The isolation of an estrone-thiol-ER complex will be conducted on a PD-10 column and characterized using MALDI and STD-NMR. About 100-150 different thiols will be used to generate the drug fragment database.

## Body

**Task-1: Establish method for in situ reaction of estrogen receptor (ER)-estrone complex with thiols (months 1-2).** *This time frame could not be followed and actual experiments took five months due to the optimization of ER-LBD protein expression and purification as the commercial ER concentration was not sufficient to carry out the proposed NMR studies.*

a. *Exchange 17-beta-estradiol with estrone in commercial ER (PANVERA).*

Commercial ER from PANVERA (currently Invitrogen Corporation) was obtained for initial testing of the suitability for NMR experiments and concentration needed for STD-NMR experiments. The supplied human-ER $\alpha$  was of molecular weight 66 kDa, isolated from recombinant baculovirus-infected insect cells (catalogue number P2187, unit size 750 pmol, unit price \$350). The protein solution was loaded on a PD10 column to exchange for a suitable buffer

for NMR experiments. It was observed that the buffers reported in the PANVERA protocol (catalogue number: P3029) for ER assay failed to elute ER from PD10 column. Hence the protein solution obtained from PANVERA (as such) was mixed with 10% D2O and subjected to a simple <sup>1</sup>H-NMR experiment using water suppression. It was observed that the concentration of the ER was too low to conduct STD-NMR experiments with the protein. It is concluded that commercial ER is expensive and its low concentration of protein makes it impossible to conduct any STD-NMR experiments with it. As a reference, human ER $\alpha$ -ligand binding domain (hER-LBD) from E.coli was used to optimize NMR buffer conditions and establish the protocol for STD-NMR experiments. hER-LBD is expressed and purified in two forms. One is Dr. Greene's protocol<sup>1</sup> wherein native hER-LBD is expressed in BL21-DE3 bacterial cells. The other protocol is from the Dr. Dino Moras group;<sup>2</sup> the high purity protein is obtained with a his6 tag which can be purified using a nickel column.

We optimized both protocols in our lab and the brief procedures are described below.

EXPRESSION AND PURIFICATION OF hER $\alpha$ -LBD (297-554): The human ER $\alpha$ -LBD (297-554) cDNA plasmid was a generous gift from Geoffrey L. Greene. The plasmid construct is shown below.

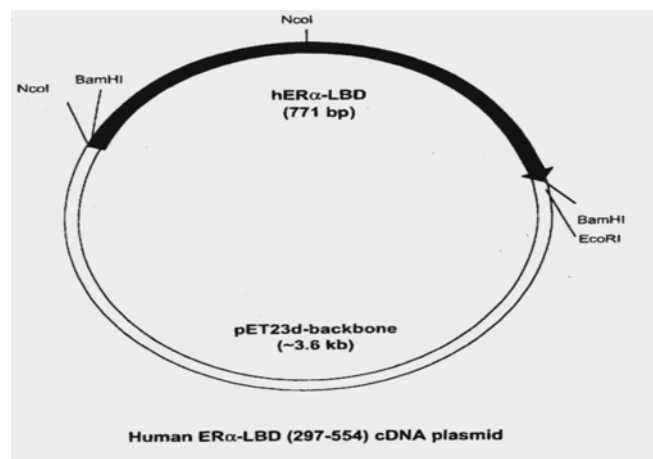


**Figure 1.** The vector containing the human ER $\alpha$ -LBD and part of the hinge region

**PLASMID EXTRACTION:** The plasmid vector, pET-23d-ERG, was employed for the expression of the desired hER $\alpha$ -LBD (the vector was obtained from Green's lab in Whatman paper). The vector was extracted by placing the Whatman paper in 50 $\mu$ l of 10mM Tris (pH 7.6) buffer. It was allowed to stand for 10 minutes after a brief centrifugation. The plasmid vector is a circular DNA which consists of the gene of interest along with other regions which help

in turning on gene expression upon adding an inducer, like IPTG (Isopropyl- $\beta$ -D-galactopyranoside). The bacterial colonies are identified on plates. The plates are prepared to contain a specified antibiotic to select for the bacteria which contain the vector that imparts an antibiotic resistance. The following steps were then taken:

1. Transformed competent *E. coli*, BL21 (DE3) pLysS was grown on LB agar plates, containing an appropriate concentration of antibiotic, carbenicillin-100µg/ml.
2. The colonies were inoculated into LB broth and incubated overnight for optimum yield. Preserved aliquots were used to culture in large quantity (1000 ml).
3. The desired gene was induced by adding 0.5mM IPTG (Isopropyl-β-D-galactopyranoside) to the above culture when the OD<sub>600</sub> reached 0.6 for four hours.
4. The culture was centrifuged after the 4-hour induction by spinning at 5000 rpm for 15 min to obtain *E. coli* pellets.
5. The cell pellet was harvested, flash frozen and stored at -80°C.
6. The cell pellet was lysed by sonication in 20mL of Lysis buffer (50mM Tris, 50mM NaCl, 1mM EDTA, 1mM DTT and 1M Urea, pH 7.4). The protease inhibitor cocktail (Sigma, P8465, 100µl), 0.1mM PMSF and 0.1mM DIFP were added before, during and after sonication.
7. The cell pellet was exposed repeatedly with a short pulse of sonication under an optimum setting for 20 sec each time until the pellet disappeared and a cloudy solution was formed.
8. The above turbid solution was centrifuged at 3200 g for 30 minutes.
9. A SDS-PAGE gel was conducted to determine the extraction of ER in supernatant. No protein was observed. The cell pellet was re-suspended in the 100 mL of lysis buffer and sonicated for three 20 sec pulses and the turbid solution was centrifuged. The supernatant still did not contain any appreciable protein with respect to the protein expressed in cells (**Figure 2**).
10. The cell pellet was suspended again but in the buffer described in Greene's paper.<sup>1</sup> The storing buffer contained 25mM Tris, 100mM NaCl, 1mM EDTA, 1mM DTT, 5M Urea, and 5% Glycerol. A SDS-PAGE gel showed that expressed ER-LBD was now present in the supernatant (**Figure 2**). The reason for extraction at higher concentration of urea solution is due to the trapping of protein in cell debris; the high concentration of urea and presence of glycerol solubilize the protein.
11. The above solution was exchanged into three different buffers using PD10 columns (explained in detail in next section). It was observed that all buffers were able to extract

ER-LBD into solution after the PD 10 column but invariably a loss of protein was observed. This could be attributed to the hydrophobicity of the ER-LBD.

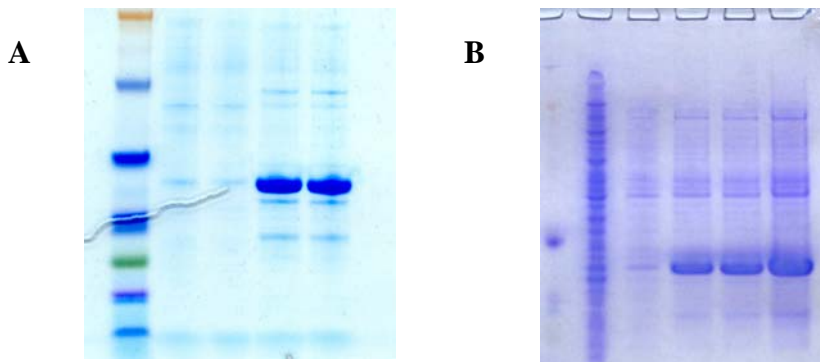


**Figure 2:** The cell lysate of ER-LBD expressed in *E.coli* from two different experiments. A) (left to right) lane 1: molecular weight marker, lane 2 & 3: protein extracted with 1M urea containing buffer, lane 4 & 5: cell debris extracted with 5M urea containing buffer. B) (left to right) lane 1: molecular weight marker, lane 2: protein extracted with buffer containing no urea, lane 3: protein extracted with 1M urea containing buffer. Lane 4 & 5: cell debris extracted with 5M urea containing buffer, lane 6: cell debris extracted with 5M urea containing buffer (2X).

EXPRESSION OF His<sub>6</sub> ER $\alpha$ -LBD: The procedure for expressing the His<sub>6</sub> ER $\alpha$ -LBD is given below.

1. The plasmid vector, pET- 15b-ER $\alpha$ -LBD, was employed for the expression of His<sub>6</sub> ER $\alpha$ -LBD and was a generous gift from Dr. Dino Moras. The vector was extracted from Whatman paper in 50 $\mu$ l of 10mM Tris (pH 7.6) buffer. It was allowed to stand for a few minutes after a brief centrifugation.
2. The extracted plasmid DNA ~2 $\mu$ l was added to the micro centrifuge tube containing 20  $\mu$ l of competent cells. The transformed competent *E. coli* [BL21(DE3)pLysS or BL21(DE3)], was grown overnight on LB agar plates kept in the incubator at 37 $^{\circ}$ C (after several days of trials the competent cell *E. coli* BL21(DE3) yielded a good number of colonies). Plating media contained an appropriate concentration of antibiotic, carbenicillin-50 $\mu$ g/ml and chloramphenicol-34 $\mu$ g/ml.
3. The colonies were inoculated in LB broth and incubated overnight for optimum yield. Preserved aliquots were used to culture in large quantity (1000 ml).

4. The desired gene was induced by adding 0.5mM IPTG (Isopropyl- $\beta$ -D-galactopyranoside), 10  $\mu$ M estradiol and 1% sucrose to the above culture when the OD<sub>600</sub> reached 0.6 for four hours.
5. The culture was centrifuged after the 4-hour induction by spinning at 5000 rpm for 15 min to obtain *E. coli* pellets.
6. The cell pellet was harvested, flash frozen and stored at -80°C.
7. The cell pellet was lysed by sonication in 20mL of Lysis buffer (2M NDSB (non-detergent sulfobetaine), 50mM NaCl, 100mM sodium phosphate pH 7.5, 10 $\mu$ M estradiol and 20 mM BME). The protease inhibitor cocktail (100 $\mu$ l), 0.1mM PMSF and 0.1mM DIFP were added before during and after sonication.
8. The cell pellet was exposed repeatedly with short pulses of sonication under an optimum setting for 20 sec each time until the pellet disappeared and a cloudy solution was formed.
9. The above turbid solution was centrifuged at 3200 g for 30 minutes. Estradiol (10  $\mu$ M) was added to the collected supernatant. The collected supernatant (40ml) was four-fold diluted (160ml) using the dilution buffer (50mM NaCl, 100mM Sodium phosphate, pH 7.5, 10 $\mu$ M Estradiol and 20mM  $\beta$ -mercapto ethanol) in order to dilute the NDSB from 2M down to 0.5M. The diluted solution was concentrated using an ultra filtration cell (Amicon YM 10) down to ~3ml. The above solution was exchanged into a Binding buffer (1M NaCl, 160mM Tris-HCl, 40mM Imidazole, pH 7.9) containing 0.1mM THP as a reducing agent. In this case, most of the protein is lost during the buffer exchange as well (**Figure 3**).
10. His Bind Quick column reagent kit (Novagen, USA) was used for purification of his6-ER-LBD using a nickel column. The following buffers are used in the purification process.
  - 80ml Binding buffer (8X= 4M NaCl, 160mM Tris-HCl, 40mM Imidazole, pH 7.9),
  - 25ml Wash buffer (8X= 4M NaCl, 160mM Tris-HCl, 480mM Imidazole, pH 7.9), and
  - 50ml Elution buffer (4X= 2M NaCl, 80mM Tris-HCl, 4M Imidazole, pH 7.9).
11. The protein purification using His Bind resin was performed at 4°C under native conditions. 1X Buffers were prepared by diluting the stock solution with deionized water. The column was equilibrated with 15ml 1X binding buffer. The sample (cell extract) was

loaded onto the column. Then column was washed with 50ml of 1X binding buffer, and was further washed with 25ml of 1X washing buffer. The protein was eluted with 10ml 1X elution buffer, and the eluent was then concentrated down to ~3.5 ml using ultra filtration (Amicon, YM 10).

12. The fractions were collected at different stages of expression and purification. These fractions were analyzed by SDS-PAGE (**Figure 3**).

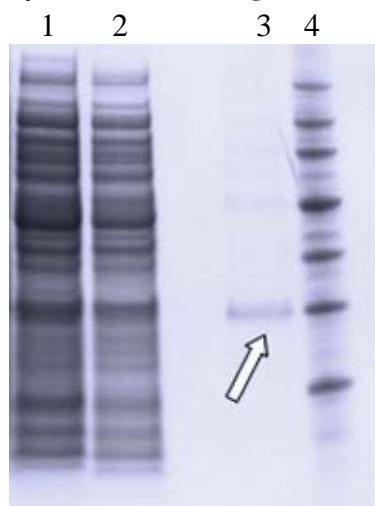


**Figure 3:** The SDS PAGE analysis showing the fractions collected during the process of expression and purification. 1. The cell extract, 2. The fraction before loading onto His-bind column, 3. Eluent from Quick Bind His column (purified protein is shown by a bold arrow). 4. Molecular marker (Novagen).

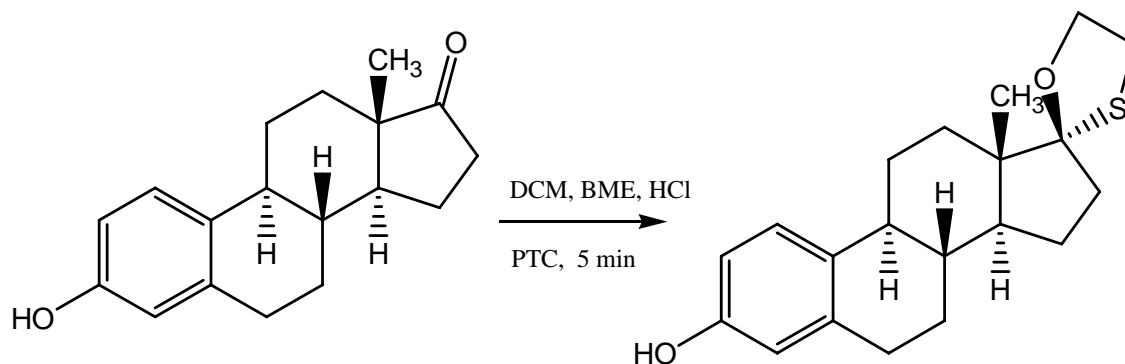
*b. Optimizing the buffer conditions for the estrone-thiol reaction.*

We performed simple reactions with estrone and an excess of  $\beta$ -mercapto ethanol (BME) in the presence of trace amounts of HCl in dichloromethane and without any catalyst in HEPES buffer (pH 7.4). The procedure for the reaction is described below (**Scheme 1**).

*Synthesis of estrone-BME adduct:* 0.1mM of estrone was dissolved in 10 mL of dichloromethane. To that, 100  $\mu$ L of 11 M HCl was added and stirred at room temperature for 10 min. 1mM BME was then added and stirred for 5 min. A phase transfer catalyst was added during the course of reaction and the precipitated product was filtered, washed with 3 mL of dichloromethane and dried under vacuum. Yield: 70%.

*Synthesis of estrone-BME adduct in aqueous buffered medium:* 0.1 mM estrone was made in a pH 7.4 100 mM HEPES buffer from a DMSO stock of estrone. To that, 1 mM BME was added and stirred for 4 hrs. The product was insoluble in an aqueous buffer and hence filtered and

purified using silica gel (240-400 mesh) column chromatography (**Figure 4 & 5**). The reaction between estrone and thiols was tested for thiols like DTT, 2-thio pyridine, 1,3-propane dithiol, 1,4 butane dithiol, etc. and in all cases the thio-hemiketal was isolated and characterized. Depending on the thiol nature either an acidic or basic catalyst was used along with phase transfer catalysts to obtain the desired hemithio ketal product.



**Scheme 1:** Reaction of estrone with  $\beta$ -mercapto ethanol in the presence of HCl and phase transfer catalyst. 1% HCl was added because it is established that 17- $\beta$ -OH of estradiol forms a hydrogen bond with His 524 (shown in Figure 1), and if this reaction is to happen inside the binding site, it may be catalyzed by the His 524 hydrogen bond.

*c. Perform the reaction by adjusting molar ratio of protein and thiol.*

10  $\mu$ M ER-LBD protein in storage buffer (25mM Tris, 100mM NaCl, 1mM EDTA, 5M Urea, 5% Glycerol, pH 7.4) was treated with 10 mM BME for 4 hours and the protein solution was submitted for MALDI. The MALDI spectrum (before and after treatment of BME) did not give any conclusive information about the formed hemi-thio ketal product. This same reaction with ER-LBD was performed with DTT and again the MALDI spectrum could not give conclusive information about the formation of adduct. This may be due to the fact that a MALDI spectrum with proteins is associated with an error  $\sim$  100 Da; most of the thiols in this proposal are within the molecular weight range of MALDI error. Hence it was concluded that MALDI could not be used for confirmation of estrone-thiol hemi ketal. Hence, another method was required to confirm the formation of the thio-hemi ketal on the ER.

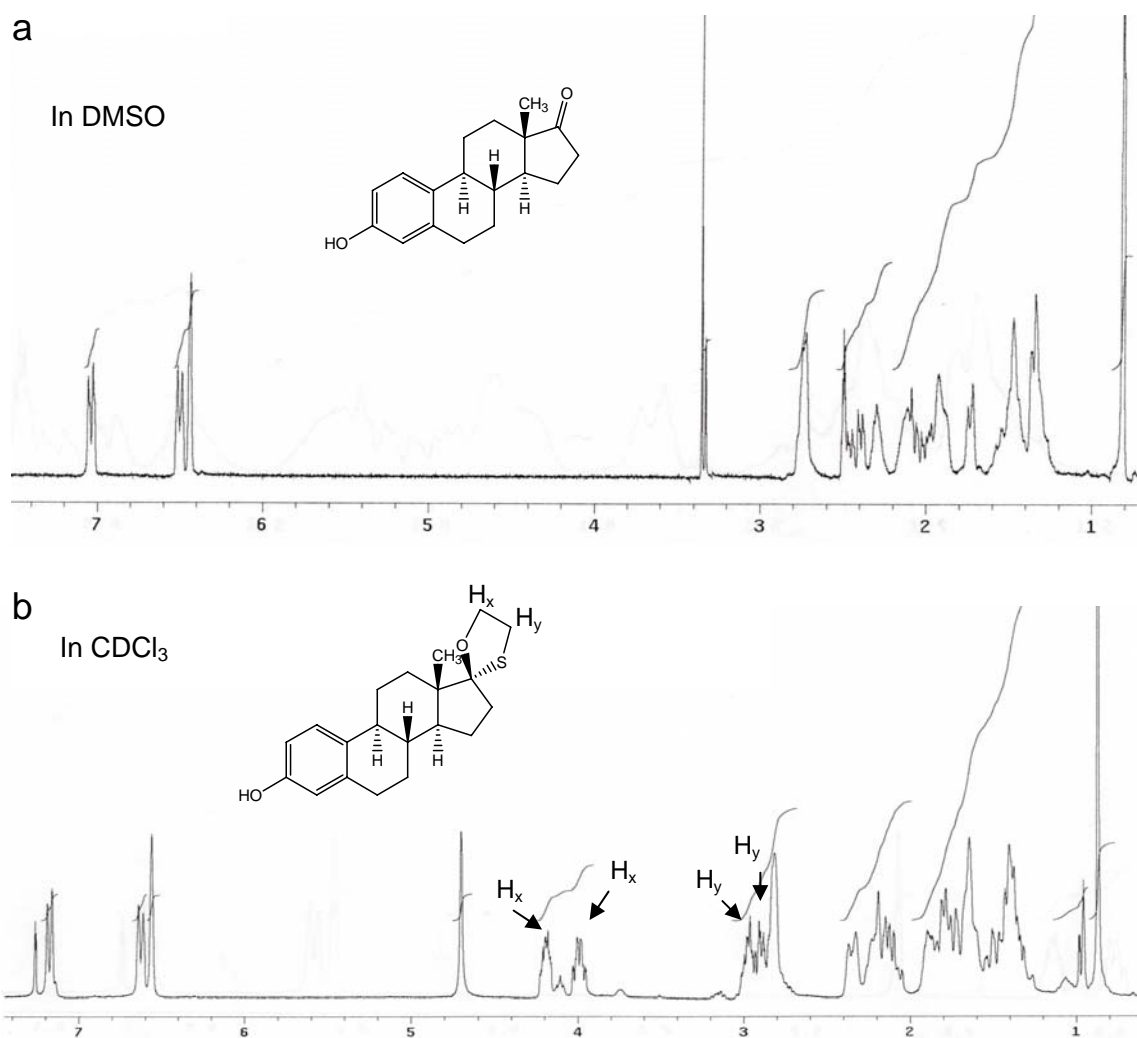


**Figure 4:** a) <sup>1</sup>H NMR spectrum of estrone in DMSO. b) <sup>1</sup>H NMR spectrum of estrone-BME adduct in CDCl<sub>3</sub>. The new NMR peaks from CH<sub>2</sub>'s of BME were marked with arrows. The cyclized product is confirmed by MALDI (expected: 330.1653, actual: 331.1153 (M+1 peak)) and the peculiar splitting pattern in <sup>1</sup>H NMR may be due to restricted orthogonal position of the two five membered rings.

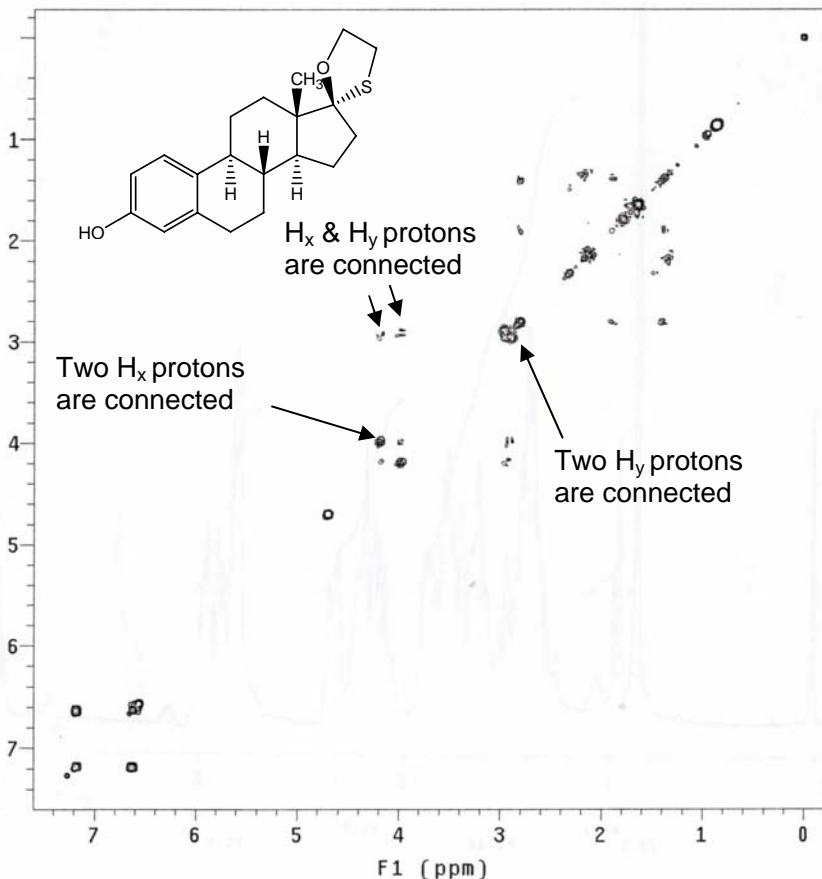


**Figure 5:** 2D-COSY spectrum of estrone-BME adduct. The cross peaks are indicated with arrows. The other stereo isomer at 17-position is synthetically not possible.

*d. Optimization of NMR buffer for ER.*

Table 1 shows the three buffers used for testing stability of the ER-LBD protein. Buffer I & II are suitable for the NMR study of ER-LBD, but obtaining a deuterated form of the buffer components is difficult and expensive. In the buffer I, deuterated *Tris* was found to be very expensive and in the case of buffer II, obtaining both *EDTA* and *Tris* in deuterated form was very expensive. Considering these, only buffer III which contained simple salts and urea was pursued for further NMR experiments. The deuterated urea was prepared by dissolving/lyophilizing urea in D<sub>2</sub>O multiple times. A proton spectrum of deuterated urea showed mild peaks of urea and these peaks were around 5 ppm (not many protein peaks appeared in this region), which would not interfere with a STD-NMR experiment. Water suppression was performed using WATER-LOGSY method and a good suppression of the water signal was observed as shown in Figure 2. The recipe of buffers employed in our study is shown.

**Table 1:**

Buffer (I) <sup>a</sup> 100 ml	Buffer (II) <sup>b</sup> 100 ml	Buffer (III) <sup>c</sup> 100 ml
50mM Tris-HCl (pH 8.0) 500mM KCl 2mM DTT 10% Glycerol pH 7.4	25mM Tris 100mM NaCl 1mM EDTA 1mM DTT 5M Urea 5% Glycerol pH 7.4	25mM KH <sub>2</sub> PO <sub>4</sub> 100mM KCl 1mM DTT <sup>d</sup> 5M Urea pH 7.4

- a. Buffer was employed according to the recipe taken from commercially available buffer.
- b. Buffer reported by Greene et al.
- c. The NMR buffer was selected to contain simple salts with a final pH feasible for NMR analysis.
- d. DTT was used to maintain protein under reduced condition and prevent dimerization of ER-LBD due to surface thiols. In actual STD experiments involving protein-thiols, the DTT free buffer was used.

**Task-2: Purification of ER-estrone-thiol complex and optimization of MALDI and STD-NMR conditions (months 3-4)** *This time frame could not be followed and actual experiments took four months due to the optimization of fluorescence polarization conditions and the re-synthesis and characterization of DSSA probe.*

a. *Optimize method for purification of ER-estrone-thiol complex using PD-10 column to separate from low molecular weight impurities.*

The expressed ER-LBD protein bound to E2 was suspended in buffer III containing 100  $\mu$ M estrone. (100  $\mu$ M estrone solution was made from 4 mM estrone stock solution in DMSO. In all of the experiments DMSO concentration was maintained below 0.1 %). A PD-10 column was used to separate protein from free estrone and estradiol. In a typical PD10 column purification procedure, protein was loaded on an equilibrated PD 10 column and the eluent was discarded. 3 mL of buffer III was used to elute protein and a simple <sup>1</sup>H NMR was obtained to identify the characteristic small molecule peaks. As mentioned previously in this report, there is a loss of protein when PD10 purification or buffer exchange was done. This could be attributed to either high retention of ER-LBD on the PD1 column or the fact that buffer III could not elute complete

protein in a PD10 procedure. We needed a low  $\mu\text{M}$  protein solution for STD-experiments and no attempt was made to refine the buffer conditions for optimum elution of ER-LBD from the PD10 column. MALDI of the ER-LBD sample before and after estrone exchange was done to get any information about the exchange estrone. The information was inconclusive. Considering the error in MALDI for a protein analysis is about one 100-200 Da, the weight difference in estrone and E2 was too small to be observed by MALDI. Hence it is not possible to identify the protein driven estrone-thiol adduct formation using a MALDI approach. We needed a different approach to identify the exchange of estrone in ER-LBD. A simple fluorescence-based approach was attempted as described in the scheme below (**Scheme 2**).

The above scheme contains a compound termed the DSSA probe.<sup>3,4</sup> We developed this probe during a different project and it was used to assay changes in concentration of cellular thiols. This probe is sensitive to mM concentration of cellular thiols and has a low reduction potential (-0.6 V). This probe was re-synthesized for this project in milligram quantities.

*b) Detection of estrone-thiol adduct formation using fluorescence polarization.*

Fluorescence polarization is a sensitive fluorescence technique in which a probe bound to a macromolecule tumbles slowly and can give rise to a fluorescence polarization signal. On the other hand a free probe which tumbles fast in the solution will not give any fluorescence polarization signal.

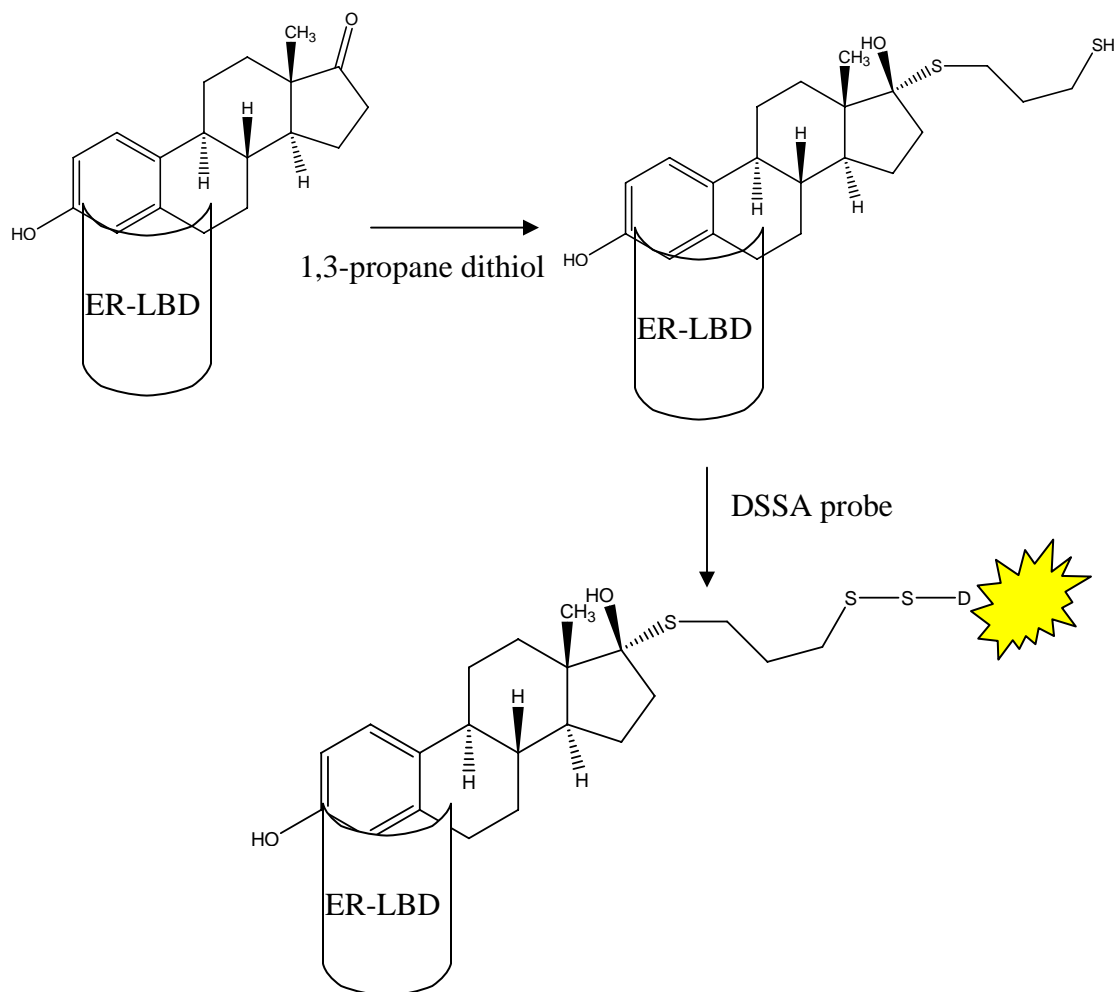
The principle behind the measurement of polarization is binding assays. The degree of polarization is given by the equation (1).

$$\text{Polarization value (P)} = \frac{\text{Intensity}_{\text{vertical}} - \text{Intensity}_{\text{horizontal}}}{\text{Intensity}_{\text{vertical}} + \text{Intensity}_{\text{horizontal}}} \quad (1)$$

Where  $\text{Intensity}_{\text{vertical}}$  is the intensity of the emission light parallel to the excitation light plane and  $\text{Intensity}_{\text{horizontal}}$  is the intensity of the emission light perpendicular to the excitation light plane.

This technique is widely used for different protein-ligand interaction studies and we recently reported a E2-analogue (E2-FITC) as a fluorescence polarization probe which localizes inside zebrafish.<sup>5</sup> The fluorescence polarization procedure followed in this project is given below.

20  $\mu\text{M}$  ER-LBD in buffer III was treated with 1 mM propane dithiol at 4  $^{\circ}\text{C}$  for 12 hours. The protein solution was separated from an un-reacted thiol using PD10 column.



**Scheme 2:** The proposed scheme of reactions for identification of estrone exchange with estradiol and validation of estrogen receptor driven inhibitor synthesis. Step 1: Reaction of estrone-thiol reaction mediated by ER-LBD. Step 2: Reaction of DSSA probe with the free thiol group to form a fluorescent product which can be detected by fluorescence polarization.

The thiol-free protein solution was assayed using 1  $\mu\text{M}$  DSSA probe. In a typical assay procedure,

1. The synthesized fluorescein compound was first tested for its effectiveness as a fluorescent probe by performing dose-response curves.
2. The DSSA sample was prepared. The DSSA probe was dissolved in DMSO and a 10  $\mu\text{M}$  stock solution was prepared in buffer III. 10  $\mu\text{l}$  of DSSA probe was added in each as well to obtain 1  $\mu\text{M}$  final concentration in the reaction.

3. The ER-LBD was prepared. The stock concentration of ER-LBD was set at 10  $\mu\text{M}$  and necessary protein dilutions were made. The protein concentration was varied from 50 nM to 5  $\mu\text{M}$ . The aliquots of protein were stored at  $-80^{\circ}\text{C}$  and thawed a few minutes prior to preparing the working stock.
4. The protein and DSSA probe solutions were mixed and the plate was incubated for one hour; the polarization was read before and after adding the probe.
5. The blank subtracted values were entered in Excel and analyzed.

The assay did not give any fluorescence polarization signal. The procedure was repeated several times by varying the temperature of the reaction, the incubation time of plate, the concentration of the DSSA probe and the ER-LBD. In all cases no fluorescence polarization signal was observed. Considering that the buffer III contains 5 M urea and is close to the protein denaturing condition, the hexa-histidine tagged ER-LBD was used.

His6-ER-LBD was exchanged to ER-working buffer (reported in PANVERA catalogue for ER $\alpha$ -assay) and the protein was treated with 1,3-propane dithiol as described above. The fluorescence polarization assay was performed for the protein after reaction with the DSSA probe. Again no fluorescence polarization signal was observed. Observation of a fluorescence signal would have indicated the reaction of dithiol with estrone and a subsequent reaction with the DSSA probe.

*c. Reasons for failure of fluorescence polarization approach and inability to confirm the estrone-dithiol reaction in presence of ER-LBD protein.*

1. There is no means to identify the exchange of estrone with ER-LBD bound E2 using any spectral technique. The STD-NMR did not work because both estrone and E2 possess nM affinity for ER-LBD, and STD-NMR can detect only mM and high  $\mu\text{M}$  (low affinity) inhibitors. The MALDI approach failed because the molecular weight difference between estrone and E2 was only 2 Daltons and is far below the resolution of MALDI.
2. The use of 5M urea in a working buffer (buffer III) probably complicated the stability of the protein. In fact, the discussions with experts in the estrogen receptor field at the American Society for Biochemistry and Molecular Biology (ASBMB) meeting, San Francisco, CA; the American Chemical Society Great Lakes Regional Meeting (ACS-GLRM), Milwaukee, WI; and the Residential School on Medicinal Chemistry (RESMED), Madison, NJ have given information that ER-LBD might exist in the proposed buffer III conditions as a mixture of active and denatured forms.

3. ER-LBD bound to E2 is a stable complex with E2 possessing about 0.2 nM Kd. We are not sure if E2 gets exchanged with estrone (Kd 5 nM).

4. We made an assumption that ER-LBD bound to estrone is formed and reacts with 1,3 propane dithiol. The DSSA probe reaction might not have worked because of the probe's low reduction potential. We observed that  $\mu\text{M}$  concentration of the DSSA probe could detect mM levels of glutathione, and that 1000 fold excess of thiol may be required for reaction with DSSA probe. We attempted this fluorescence polarization approach considering its sensitivity and still the approach failed.

**Task-3: Analysis of 150-200 commercially available thiols with estrone-ER complex using MALDI and STD-NMR (Months 5-10).**

We purchased a set of 104 thiol fragments but could not perform any STD-NMR experiments for estrone-thiol reaction in the presence of ER-LBD due to a lack of a sensitive technique for monitoring the progress of the reaction and identification of the final product. Competitive STD experiments will be attempted in the future.

**Task-4: Chemical synthesis of potential estrone-thiol compounds and determination of their binding affinities against ER using fluorescence binding assay (Month 11).**

An estrone-thiol reaction in the absence of protein was found to proceed smoothly both in organic solvents and in an aqueous buffered medium. We synthesized a few estrone-thiol adducts for initial studies and for proof of concept. No further synthesis of derivatives was performed due to time constraints on the project.

**Task-5: Development of database of drug fragments with specific agonist/antagonist interactions and proposal of a SAR model. Refine the SAR model with the help of docking studies and publish the results (Month 12). *This time frame could not be followed and actual experiments took three months due to the optimization of ER-LBD protein docking and database development.***

Our group is involved in the development of fragment databases for different proteins and we used a novel approach to construct a thiol-fragment database for ER-LBD. The idea is that if there is a reaction between ER-LBD bound estrone and a thiol and if the thiol is situated close to the binding site and if by docking, we can determine the preference of thiols for agonist vs. antagonist preference, a thiol fragment database for ER-LBD could be constructed. This is the aim of this proposal - constructing a thiol fragment database which could give information about

agonist/antagonist preference with which future experiments can be directed towards synthesizing compounds with selective ER-agonist/antagonist activity in specific tissues.

*Docking studies:* The crystal structures of human ER $\alpha$ -LBD isoforms (both agonist and antagonist) were minimized using an AMBER force field using Molecular Operating Environment (MOE) software. ADT (Autodock Tools) software was used to prepare the protein structures for docking calculations by adding partial charges, solvation parameters and polar hydrogens. The agonist and antagonist structures were overlaid using Deep-View software (after removing raloxifene from human ER  $\alpha$  antagonist) in order to bring estradiol in the binding site of an ER $\alpha$ -LBD antagonist structure. These structures were converted to 3D coordinates using CORINA and integrated into a Pipeline Pilot (Scitegic, Inc.) protocol which converts the structure into a Z-Matrix. Finally, the structures were minimized using AM1 semi-empirical calculation under Gaussian. The structures were docked in both states (agonist vs. antagonist) using Autodock 3.0 software. The grid box size is flexible. The one used for Figure 5 was constructed around the O17 coordinates of estradiol and had a size of 0.175 Å \* 60 grid points in xyz co-ordinates.

*ER-LBD bound to estradiol with agonist/antagonist conformation.* In a typical docking approach, the ER-agonist (1ERE) and ER-antagonist (1ERR) were obtained from PDB. In the ER-antagonist, the raloxifene was replaced by E2 and the structure was minimized with the new ligand (E2). Then a database of 104 thiol fragments (which we purchased from Aldrich) was docked and the low energy structures were identified.

*The Thiols:* The source of thiols used in this study (total 98) was part of a 94,426 member commercial screening collection, available in SD format (From Aldrich screening collection and Aldrich fragment database). Using Pipeline Pilot chemo informatic software, all thiols were selected and parsed based on total formal charge, which is needed for Gaussian AM1 calculations. Conversion of SD format structures to optimized 3D structures was accomplished by first calculating crude 3D structures using CORINA, then calculating the pKa and correct ionization state. At this point, optimized 3D structures could be calculated for all 98 thiols, using Gaussian.

*Scoring thiols for druglike nature:* “Druglike” has been defined in this study by using a database of 5,223 drugs to build a Bayesian model, and using this model to calculate a Druglike Score. Values range from -60 to +50, with any value above 0% being reasonably druglike. One widely

used measure of druglike nature is adherence to the Lipinski “Rule of 5”.<sup>6</sup> and all the drug fragments selected obeyed this rule.

*The thiol Database:* All docked structures and calculated properties for the 98 thiol fragments used in this study can be viewed in the thiol database, available at [www.marquette.edu/cpfm](http://www.marquette.edu/cpfm).

The database contains the following information for each thiol: (a) structures as 2D representations (gif images), (b) structures as 3D representations (AM1 minimized), viewed by clicking on the 2D gif images, using any structure viewing browser plug-in (RasMol, the MDL<sup>®</sup> Chime Plug-in, Cambridge Soft Chem3D Net Plugin), (c) vendor catalog number, (d) pKa value(s) and ionization site name(s), (e) calculated Druglike Score, (f) AutoDock energies in kcal/mol for agonist conformation (tighter binders have the most negative values), (g) AutoDock energies in kcal/mol for agonist conformation (tighter binders have the most negative values) which is clickable to show that pose relative to ER-LBD helices 11 and 12, (h) recalculated binding energy from X-Score (multiply by -1.36 to convert to a binding energy), (i) index number, which is clickable to view all 10 poses from the docking in agonist conformation, and (j) index number, which is clickable to view all 10 poses from the docking in antagonist conformation,

*Orientations of thiol reductants inside binding site:* A simple result of the fragment database study for preference for agonist/antagonist orientation, the orientations and binding energies of two commonly known thiol fragments and thiol reductants DTT and BME were shown. Thiol reductants were docked with ER-LBD and for the most stable 3D structure, energies and distances were calculated. These results suggested that ER-agonist/antagonist orientation has different interactions with different thiols and that these interactions are not dictated by any structural constraints. This conclusion was made based on the docking energies and the binding pattern of diverse set of 98 thiols set. Based on binding energies and distance between E2 and thiol (**Table 2**), DTT was observed to prefer the antagonist form and it has a stable docked energy of -3.22 Kcal/mole compared to an agonist energy of + 1.26 Kcal/mole. Also, DTT antagonist and agonist orientations are almost perpendicular to each other (**Figure 6**) and the antagonist is closer to the C17 on estrone ring. *If we overlay **Figure 7c & d**, there is perpendicular orientation between E2 and raloxifene bound to ER-LBD. This observation has never been proposed as a probable reason for agonist/antagonist switch.* If estrone is present in ER-LBD, C17 is the carbon position where thiols will react. Thus, the distance between C17 of

estrone and S on thiol is important. The distance between C17 of estrone and S on DTT is 4.93 Å compared to agonist orientation of 5.36 Å. BME seems to have similar stabilizing interactions in the presence of an agonist and an antagonist based on the docked energy calculations. BME has -1.85 and -2.67 Kcal/mol energy for an agonist and antagonist respectively and this difference is reflected in their C7 to S distances similar to DTT (**Table 2**). *This observation of simple thiol reductants with few structural differences yet having large differences in their orientation, binding energy and distances is of interest and further studies in this direction need to be conducted. The understanding of the agonist/antagonist preference for simple thiol fragments has to do with the specific amino acids for the switch between agonist and antagonist and could be understood by molecular biology studies involving mutations in the ER-LBD binding site sequence.*

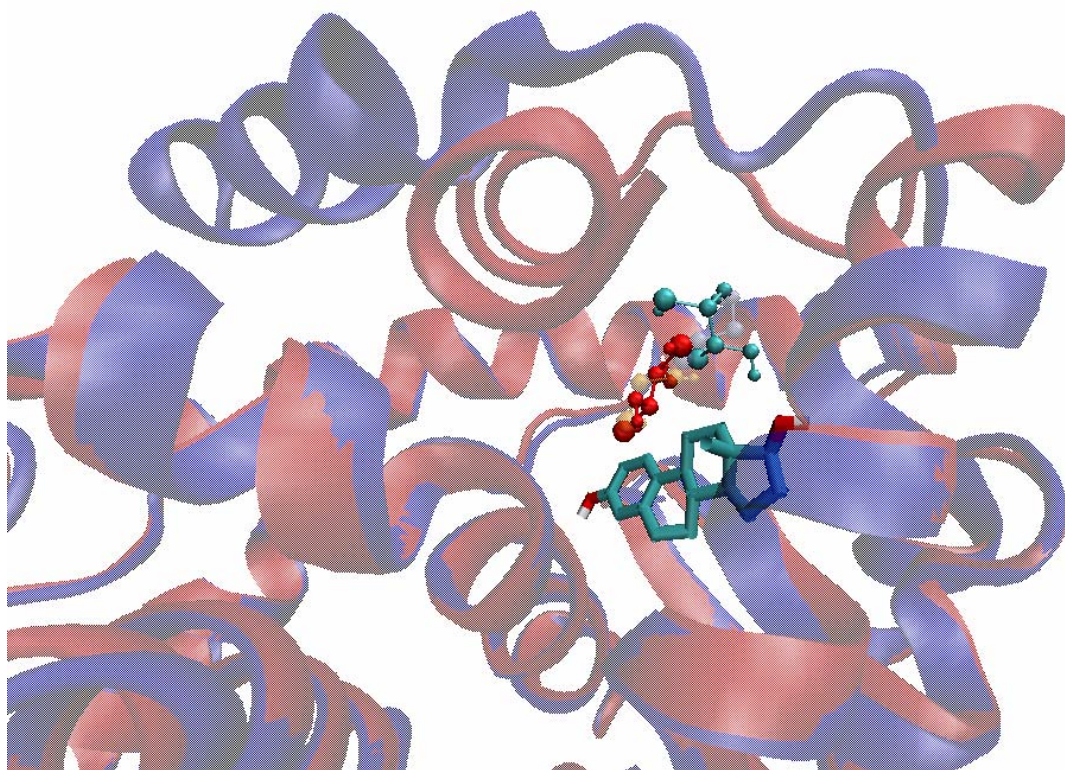


**Figure 6:** Overlay of the binding site for human ER  $\alpha$  agonist – 1ERE (red) and human ER  $\alpha$  antagonist –1ERR (blue) structures, with the estradiol kept in the binding pocket and the position of DTT after it was docked in the agonist form (red) vs. antagonist form (cyan). The perpendicular orientation of DTT in antagonist form with respect to agonist form clearly suggests that there are different stabilizing interactions for antagonist vs. agonist and can be studied using *in silico* methods.

**Table 2:** The docked energies and distances of thiol reductants docked with ER-LBD in agonist and antagonist form.

Thiol	Dist (Å) C17-S agonist	Dist (Å) C17-S antagonist	Docked Energy (Kcal/mol) ER-agonist	Docked Energy (Kcal/mol) ER-antagonist
BME	5.65	5.23	-1.85	-2.67
DTT	5.36	4.93	+1.26	-3.22

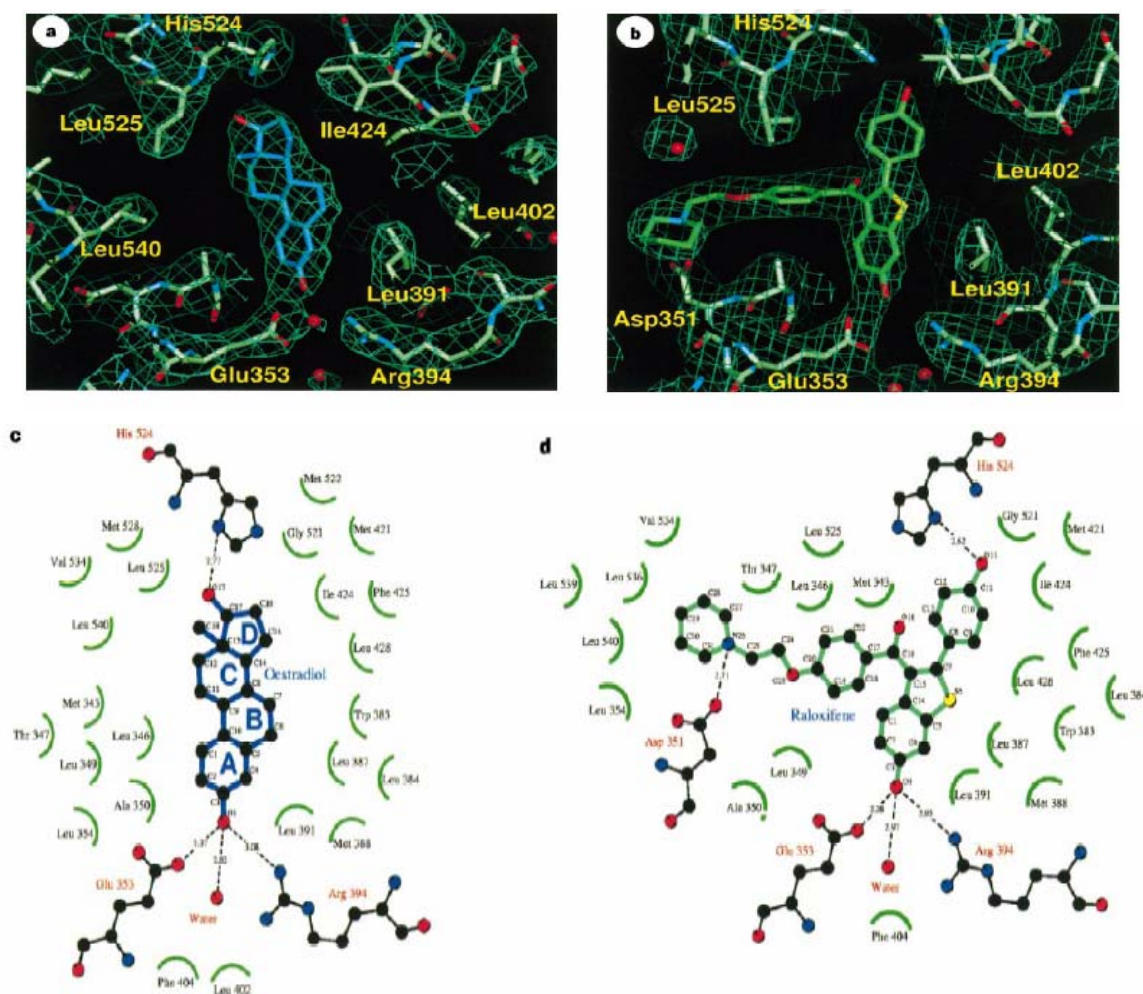


**Figure 7:** a) Crystal structure of E2 bound to ER-LBD, showing proximal amino acid residues; b) Crystal structure of raloxifene bound to ER-LBD, showing proximal amino acid residues; c) for E2, the key interactions with His 524 and Arg 394 are depicted by dotted lines; d) for raloxifene, the key interactions with His 524 and Arg 394 are depicted by dotted lines. Note that in c and d, the Arg 394 hydrogen bond interactions are the same, while His 524 rotated by 180°.

## Key research accomplishments

- We developed a database of thiol fragments in agonist/antagonist conformation with 17- $\beta$ -estradiol (E2) bound estrogen receptor-ligand binding domain (ER-LBD). The database is publicly available at [www.marquette.edu/cpfm](http://www.marquette.edu/cpfm) and has clickable fields in it which provide a view of the orientations of different thiols along with E2 bound to ER-LBD. The Druglike Score, in comparison with Lipinski rule of 5, is provided in the database for different thiols. *We are in process of docking 2,620 thiols (both drug fragments and commercially available thiols) using the above strategy and the results will be posted at [www.marquette.edu/cpfm](http://www.marquette.edu/cpfm).* This information is invaluable for thiol fragment selection for drug discovery purposes. The information in this database could drive synthesis of estradiol-analogues with ER-agonist/antagonist activity in the presence of specific tissues.
- We attempted an NMR approach and realized that NMR study of this 33 kD protein is not simple. The near denaturing conditions of 5M urea in the buffer have made the stability of protein complicated. In fact, our study points out that the reported conditions for storing this protein are not validated in terms of how much protein is in an active conformation, and the long term stability in these near denaturing conditions is not known.
- MALDI could not be used for ER-LBD bound estrone-thiol complexes because the error in MALDI (about 100-200 Da) would not detect the difference in mass between estrone and estrone-thiol complex.
- We could not achieve the enzyme driven inhibitor synthesis protocol for the estrogen receptor-estrone pair, but devised a useful fluorescence polarization-based approach. Though this approach was unsuccessful for ER-LBD, it can be applied for other protein-ligand complexes and could be used as a useful tool for potential ligand screening, after further optimization.
- As exemplified with DTT and BME docked to ER-LBD, the different orientation preferences for these common thiols with respect to protein binding is of definite interest and could provide useful input for selective antagonist/agonist synthesis and could ultimately lead to new drugs with minimal side effects. This study could be a starting point for designing a new generation of selective estrogen receptor modulators (SERMs).

- If the binding of DTT and BME in estradiol bound estrogen receptor is occurring, then this could have large implications of the steroidal biochemistry of estrogen receptors. This study also points out that some of the biochemical results obtained using thiol reductants like DTT and BME with ER-LBD need to be studied with non thiol reductants like TCEP and THP.
- The loss of ER-LBD protein during PD10 buffer exchange is of concern and also of biochemical interest suggesting the hydrophobicity of ER-LBD is not completely understood.

### Reportable Outcomes

1. Phani Kumar Pullela, Aurora D. Costache, Daniel S. Sem. “Effect of thiol reductants on estrone and estrogen receptor” *American Society for Biochemistry and Molecular Biology (ASBMB)* annual meeting, **2006**, San Francisco, CA.
2. Phani Kumar Pullela, Taurai Chiku, Michael J. Carvan, Daniel S. Sem. “Fluorescence-based detection of thiols in vitro and in vivo using dithiol probes”. *Analytical Biochemistry*. 352 (**2006**), 265-273.
3. Phani Kumar Pullela, Taurai Chiku, Daniel S. Sem. Small molecule tools for intracellular-thiol quantitation. *American Chemical Society-Great Lakes Regional Meeting (ACS-GLRM)*, **2006**, Milwaukee, WI.
4. Taurai Chiku, Phani Kumar Pullela, Daniel S. Sem. A dithio coupled kinase and ATPase assay. *Journal of Biomolecular Screening*. **Accepted for Publication**.
5. **Thiol database** [www.marquette.edu/cpfm](http://www.marquette.edu/cpfm).

### Conclusion

- The proposed study in this grant was partially successful. We were able to design a database with thiol fragments with selectivity for agonist/antagonist in presence of estradiol, which could serve as a useful starting point for the ultimate design of molecules in the presence of selective tissues. This agonist/antagonist design in the presence of tissues is the ideal way to obtain selective ER agonist/antagonists. We failed to optimize reaction conditions for estrogen receptor driven inhibitor synthesis. The uncertainty about the estrone binding to ER-LBD has forced us to employ an alternate approach to MALDI, namely fluorescence polarization (FP). The FP-based approach developed for detection of protein inhibitors and monitoring protein driven inhibitor synthesis was novel but

failed to provide any valuable information. This FP-based approach could be applied to new protein-ligand systems and might find good use in future drug discovery. Finally, we demonstrated that DTT and BME have different orientations when bound to ER-LBD/estradiol complex, based on docking calculations. These results could have interesting implications for steroidal biochemistry as well as estrogen receptor-ligand synthesis. *We are in process of docking 2,620 thiols (both drug fragments and commercially available thiols) using the above strategy and the results will be posted at [www.marquette.edu/cpfm](http://www.marquette.edu/cpfm).*

*Future work:*

1. It is imperative to evaluate the stability of the estrogen receptor in near denaturing conditions and if unstable, the ratio of stable versus denatured protein in the given buffer condition must be determined before attempting any further NMR experiments.
2. The thiol fragment docking data with E2 bound ER-LBD needs to be experimentally verified using STD-NMR. In this case, STD-NMR could be able to identify the mM or possible  $\mu$ M inhibitors. The linking of estradiol with appropriate thiol fragments could give more potent and selective inhibitors for ER.
3. The interesting binding patterns of simple thiol reductants with ER-LBD needs to be experimentally verified using STD-NMR and implications for steroidal biochemistry be determined.
4. The fluorescence polarization-based protein driven inhibitor detection method involving DSSA probes is interesting and could have potential drug discovery applications. This needs to be studied with other protein systems.
5. It is important to explore ER from other organisms, considering the solubility issues with the human ER. Just prior to the start of this project, we reported<sup>5</sup> that zebrafish ER is similar (about 90 % in LBD region and 55% overall) to human ER and directing the above studies with this protein could improve solubility issues and facilitate NMR studies.

*“So what section”:*

The study is aimed at finding protein driven inhibitor synthesis tools for estrogen receptor, one of the difficult and complex proteins in biochemistry. The development of a thiol fragment database

for ER-agonist/antagonist preference is novel and could aid future drug discovery in this field. The buffer suitability and stability problems with ER are of definite interest and need to be addressed before any NMR studies are attempted. The biochemical data available today about estrogen receptors needs to be translated for drug discovery purposes. The possibility of a near binding site for thiol fragments (or any other class of fragments like amines, etc.) needs to be explored, which could permit the specific tissue selectivity in inhibitor design, which is the ultimate direction of this proposal.

### **Personnel**

Dr. Phani Pullela is the only person who received pay from this research effort.

## References

1. Seilstad DA, Carlson KE Katzenellenbogen JA, Kushner PJ, Greene GL. Molecular characterization by mass spectrometry of the human estrogen receptor ligand binding domain expressed in *Escherichia coli*. *Mol. Endocrinol.* **9**, 647-658 (1995).
2. Eiler S, Gangloff M, Duclaud S, Moras D, Ruff M. Over expression, purification and crystal structure of native ER alpha LBD. *Protein Expr. Purif.* **22**, 165-173 (2001).
3. Pullela PK, Chiku T, Caravan III MJ, Sem DS. Fluorescence-based detection of thiols *in vitro* and *in vivo* with DSSA probes. *Anal. Biochem.* **352**, 265-273 (2006).
4. Chiku T, Pullela PK, Sem DS. A dithio coupled kinase and ATPase assay. *J. Biomol. Screen.* **2006** [accepted].
5. Costache AD, Pullela PK, Kasha PC, Sem DS. Homology modeled ligand-binding domains of zebrafish estrogen receptors  $\alpha$ ,  $\beta_1$ , and  $\beta_2$ : from *in silico* to *in vivo* studies of estrogen interactions in *Danio rerio* as a model system. *Mol Endocrinol.* **19**, 2979-2990 (2005).
6. Lipinski CA, Lombardo F, Dominy BW, Feeney PJ. Experimental and computational approaches to estimate solubility and permeability in drug discovery and development settings. *Adv. Drug. Deliv. Rev.* **46**, 3-26 (2001).
7. Brozowski AM, Pike ACW, Dauter Z, Hubbard RE, Bonn T, Engstrom O, Ohman L, Greene GL, Gustaffson JA, Carlquist M. Molecular basis of agonism and antagonism in the oestrogen receptor. *Nature* **389**, 753-758 (1997).

## Appendices

**American Chemical Society-Great Lakes Regional Meeting, Milwaukee, WI**

**Wednesday, 31 May 2006 - 2:50 PM**

### **Small Molecule Tools for Intracellular-Thiol Quantitation**

**Phani Kumar Pullela** and Daniel Sem. Marquette University, Milwaukee, WI

Thiol containing compounds are essential for proper function of a cell. The levels of thiols determine the redox-potential, oxidative stress, and disease state of a cell. In vivo quantitation of thiols is achieved by genetically encoded green fluorescent protein (GFP), which relies on fluorescence resonance energy transfer (FRET) with nearby amino acid residues or other fluorescent peptides. This strategy has a significant drawback; the unavailability of GFP encoded systems for all protein and cell types. For redox measurement inside cells, small molecule probes are not available, except for bromobimanes, but they have a high redox potential which tend to oxidize the intracellular environment. We recently demonstrated that DSSA dithiol probes with unusually low redox potential and high cell permeability can be an option for intracellular quantitation of thiols. But these probes are based on fluorescence quenching and for redox potential measurement and intracellular applications; probes that show FRET are preferred. Hence, we report two FRET based disulphide derivatives for quantitation of thiols. The coumarin-FITC disulphide FRET pair is synthesized from reaction of 7-mercapto-4-methyl coumarin and 4-aminophenyl disulphide, and condensation of that disulphide with FITC. The biophysical characterization of this compound clearly demonstrates its wide applications in biochemistry, apart from redox potential measurement and intracellular quantitation. We also developed a fluorescein-rhodamine disulphide FRET pair but charge on rhodamine precludes its intracellular application. But this compound's FRET ability enables many biochemical applications like, enzyme assays, in vitro quantitation of thiols and glutathione quantitation etc. This FRET pair was synthesized by insertion of a piperazine group on rhodamine B to prevent the familiar amide cyclization to a lactam form. This research was supported in part by Department of Defence-Breast Cancer Concept Award # W81XWH-05-1-0476.

## Fluorescence-based detection of thiols in vitro and in vivo using dithiol probes

Phani Kumar Pullela<sup>a</sup>, Taurai Chiku<sup>a</sup>, Michael J. Carvan III<sup>b</sup>, Daniel S. Sem<sup>a,\*</sup>

<sup>a</sup> Chemical Proteomics Facility at Marquette, Department of Chemistry, Marquette University, Milwaukee, WI 53201, USA

<sup>b</sup> Great Lakes WATER Institute and Marine and Freshwater Biomedical Sciences Center, University of Wisconsin–Milwaukee, Milwaukee, WI 53204, USA

Received 20 December 2005

Available online 20 February 2006

### Abstract

Thiols play a central role in maintaining biological homeostasis. Their levels can change dramatically in response to oxidative stress associated with toxic insults, bacterial infection, and disease. Therefore, a reagent that can monitor thiol levels both in vitro and in vivo would be useful for assays and as a biomarker. Such a reagent should (i) be selective for thiols, (ii) be able to penetrate cell walls, and (iii) have a low reduction potential so as not to create oxidative stress in a cell. We have developed such a fluorescent reagent (DSSA) based on a dithiol linker: (i) the use of a dithiol linker makes it selective for thiols; (ii) the use of fluorophores that populate neutral states at physiological pH improves cell wall penetration; and (iii) because of the reagent's low reduction potential (−0.60 V), it will not stress cells oxidatively. For example, 5 μM of reagent is responsive to changes in glutathione levels in the physiologically relevant range of 1 to 10 mM, yet this would oxidize less than 1% of cellular glutathione. In *Escherichia coli*, decreased thiol levels were detected in cells deficient in glutathione synthesis. In zebrafish embryos, the DSSA reagent permitted detection of unusually high thiol levels in the zebrafish chorion.

© 2006 Elsevier Inc. All rights reserved.

**Keywords:** Thiol; Fluorescence assay; Disulfide; *Escherichia coli*; Zebrafish

Thiols play an important role in biochemistry, both as components of protein structures and as metabolic intermediates. The most abundant cellular thiol is reduced glutathione (GSH),<sup>1</sup> which plays a central role in combating oxidative stress and maintaining redox homeostasis [1]. GSH is able to create a reducing environment in the cytosol of both eukaryotes (−0.23 V) and prokaryotes (−0.27 V) [2], and this redox state will be reflected in the overall level

of cellular thiols (all R<sub>i</sub>–SH) because thiols exist in a redox equilibrium between mercaptan and disulfide forms (2R<sub>i</sub>S<sup>−</sup> ⇌ R<sub>i</sub>S – SR<sub>i</sub>). But the thiol redox state is not expected to be uniform in a cell. For example, the endoplasmic reticulum of eukaryotes is more oxidizing than the cytosol, and large cellular redox state changes often are associated with disease [3]. But the extent of the variability of the thiol redox state within different cellular microenvironments is not well understood because there are no in vivo fluorescent probes available that can penetrate cell walls and selectively label thiols without causing oxidative or other cellular damage. Such a probe would need to (i) be neutral to permit cell wall penetration, (ii) be dithiol based to permit maximum thiol selectivity, and (iii) have a low reduction potential so as not to stress the cell oxidatively.

The most widely used reagent for measuring thiol levels is Ellman's reagent [4]. But this reagent is useful

\* Corresponding author. Fax: +1 414 288 7066.

E-mail address: [daniel.sem@mu.edu](mailto:daniel.sem@mu.edu) (D.S. Sem).

<sup>1</sup> Abbreviations used: GSH, reduced glutathione; GFP, green fluorescent protein; GSSG, oxidized glutathione; BOP, benzotriazol-1-(yl)oxytris(dimethylamino)phosphonium hexafluorophosphate; FITC, fluorescein 5-isothiocyanate; TLC, thin-layer chromatography; NMR, nuclear magnetic resonance; MALDI, matrix-assisted laser desorption ionization; DTT, dithiothreitol; TCEP, tris(2-carboxyethyl)phosphine hydrochloride; LB, Luria–Bertani; DMSO, dimethyl sulfoxide; FRET, fluorescence resonance energy transfer.

only in vitro because its charge precludes membrane crossing and because absorbance-based assays are not practical for measurements inside cells. Commercially available fluorescent thiol probes include maleimide, iodoacetamide, and methyl bromide-conjugated bodipy [5], all of which have been used for labeling thiols in cellular protein extracts [6,7]. But because these probes are based on nonspecific electrophiles, they are inherently less selective than dithiol-based probes. Other disadvantages are that (i) they permanently label thiols and so cannot respond to dynamic fluctuations in thiol levels in a living cell and (ii) they are not useful for real-time thiol assays because reaction with thiols does not produce a fluorescence change. Although bromobimanes [8] are highly reactive toward cellular thiols, their high reduction potential makes them nonoptimal for intracellular applications [9]. The most promising strategy so far for measuring thiols in vivo was presented by Dooley and coworkers using a green fluorescent protein (GFP) indicator [10]. But that approach required the genetic introduction of the GFP-based thiol sensor.

In this article, we present fluorescent dithiol (DSSA) probes for detecting thiols both in vitro and in vivo. The design of the DSSA probe builds on a reagent recently reported by Adamczyk and Grote [11], with fluorescein (D, donor) and rhodamine (A, acceptor) tethered in the same molecule. Because rhodamine is fluorescent at low pH (<6.0) and fluorescein is fluorescent at high pH (>6.0), their reagent was fluorescent over a wide pH range. Important properties of their probe were that (i) it avoids any differential permeability of the fluorophores by covalently tethering them and (ii) the cycliza-

tion of fluorescein to a neutral spirolactone (at pH < 6.0) and rhodamine to a neutral spirolactam (at pH > 6.0) ensures membrane permeability [11–14] at intermediate pH values.

We have developed analogous probes that join fluorescein and rhodamine by a dithiol linkage that can be selectively cleaved by thiols (Fig. 1A). This probe not only will penetrate cell walls and label thiols in vivo with both fluorescein and rhodamine (Fig. 1B) but also has the added advantage of permitting real-time thiol-based assays in vitro and in vivo because separation of the two fluorophores leads to a large increase in fluorescence for fluorescein (Fig. 1A). Therefore, the heterosubstituted probes presented herein have advantages over homosubstituted probes such as didansyl and dibodipy cystine [5], which give only small fluorescence changes on thiol reduction and show no absorbance changes. Finally, the unusually low reduction potential of the DSSA probes means that they will not oxidize cells. It also means that they can be used at low concentrations ( $\mu\text{M}$ ) and still be responsive to changing thiol levels in the millimolar range; this is relevant because cellular glutathione is present in the 5- to 10-mM range, with GSH/oxidized glutathione (GSSG) ratios varying from 100:1 to 300:1 [2,15,16].

## Materials and methods

### Reagents

All biochemical reagents were obtained from Sigma, and all synthetic reagents were obtained from Aldrich. *Esche-*

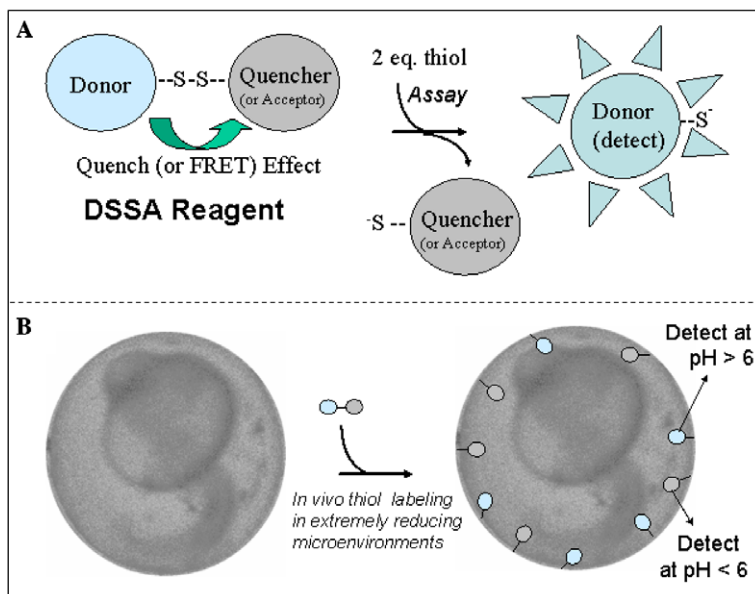


Fig. 1. Schematic representation of thiol detection with DSSA probes. (A) Probe use in an assay where an increase in fluorescence is monitored due to removal of quenching or a decrease in FRET is monitored due to removal of an acceptor. (B) The neutral probe is able to penetrate cell membranes and label intracellular thiols with both fluorescein (fluorescent at pH > 6.0) and rhodamine (fluorescent at pH < 6.0). At typical probe concentrations (<10  $\mu\text{M}$ ), labeling is selective for extremely reducing microenvironments such as reductants with  $E^{\text{red}} \leq -0.3$  V which are present at greater than 1 mM.

*richia coli* Origami(DE3)pLysS cells [17], as a glycerol stock, and BL21(DE3)pLysS competent cells were obtained from Novagen.

### Synthesis of the DSSA probes

The DSSA probe with an aromatic linker was prepared (Fig. 2A) from 1 mmol of diaminophenyl disulfide dissolved in a 4:1 acetonitrile/chloroform mixture, to which 0.3 mmol rhodamine B in acetonitrile was added. Reaction was initiated by the addition of 0.31 mmol BOP (benzotriazol-1-(yloxy)tris(dimethylamino)phosphonium hexafluorophosphate) reagent and 20 mmol triethylamine and stirred for 15 h at room temperature. The amide was purified

by silica gel (230–400  $\mu$ ) column chromatography using 20% ethyl acetate in hexane (yield = 46%). The 0.1 mmol amide was reacted with 0.12 mmol fluorescein 5-isothiocyanate (FITC) in acetone at room temperature for 16 h. The final DSSR<sub>Ar</sub> probe was purified by silica gel (230–400  $\mu$ ) column chromatography using 30% hexane in ethyl acetate and then by preparative thin-layer chromatography (TLC, percentage yield = 13%). All of the above reactions were done in the dark, and all compounds were characterized by <sup>1</sup>H nuclear magnetic resonance (NMR), <sup>13</sup>C NMR, and matrix-assisted laser desorption ionization (MALDI). <sup>1</sup>H NMR (acetone-*d*<sub>6</sub>): 9.6 (s, 1H), 9.4 (s, 1H), 9.1 (s, 1H), 8.2 (1H), 7.9 (2H), 7.5 (6H), 7.3 (2H), 7.1 (1H), 7.0 (3H), 6.6 (8H), 6.4 (2H) 6.3 (2H), 3.4 (8H), 1.1 (12H).

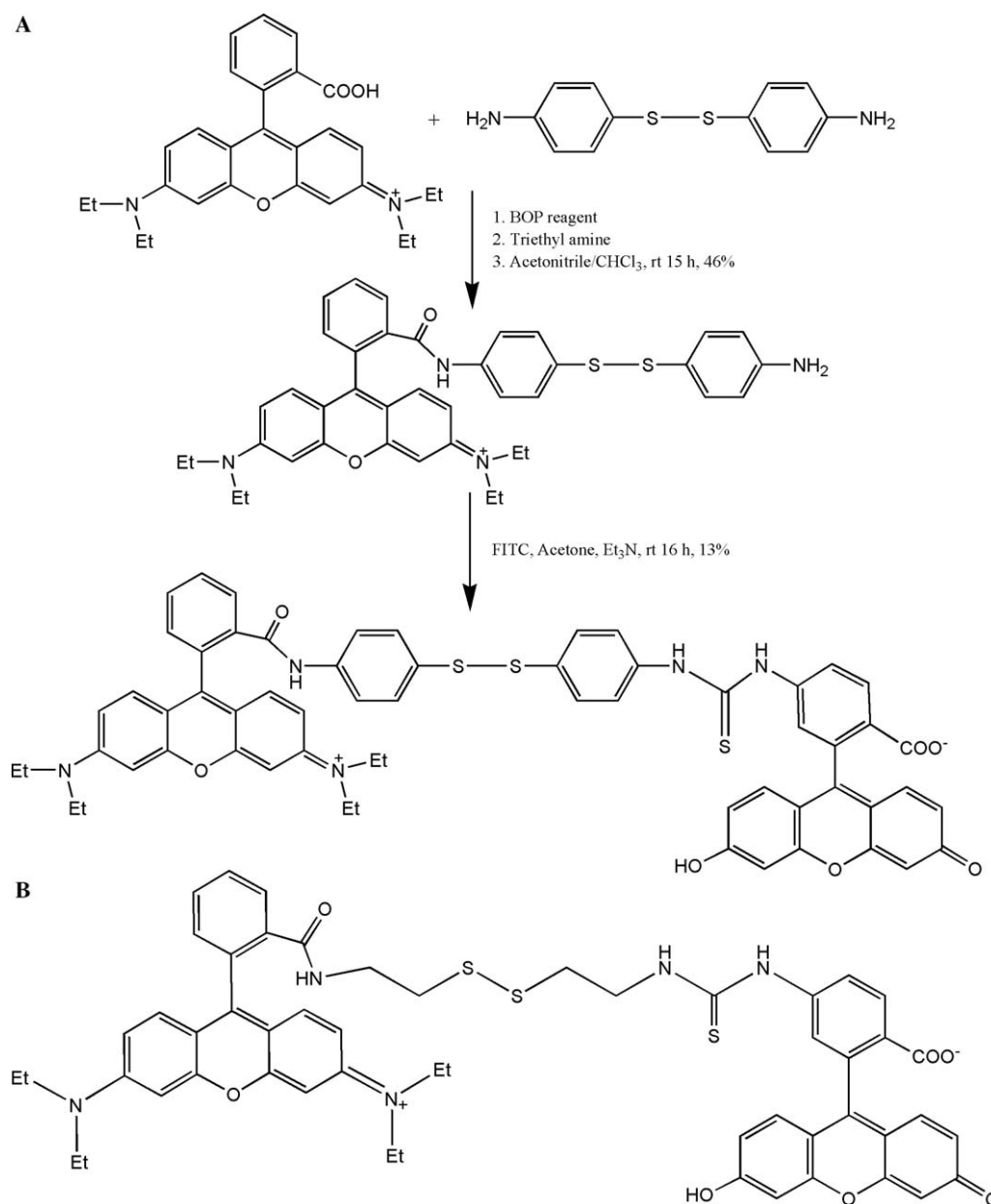


Fig. 2. (A) Synthesis of the asymmetric dithiol fluorescent probe with an aromatic linker (DSSA<sub>Ar</sub>). (B) Synthesis of the analogous probe with an aliphatic linker (DSSA<sub>Al</sub>) was done in the same manner but instead starting with cystamine and conjugating the fluorophores to cystamine's two amino groups.

$^{13}\text{C}$  NMR (acetone- $d_6$ ): 205, 180, 169, 167, 160, 154, 153 (two peaks), 149, 141, 139, 138, 134 (three peaks), 131, 130, 128 (six peaks), 124 (three peaks), 119, 113, 111, 109, 106, 104, 102, 98, 44, 12. Mass 1062.72 (expected  $M^{+} = 1062.30$ ).

The version of the DSSA probe with an aliphatic linker (DSSA<sub>Al</sub>) was prepared as described above but using cystamine dihydrochloride rather than the diamino-phenyl disulfide as starting material (Fig. 2B). In this case, DSSR<sub>Al</sub> yield was 17%. Mass 1002.77 (expected  $M^{+} = 1002.49$ ).

#### *In vitro* fluorescence studies of thiol reactivity

The buffers used in the pH study (Fig. 3) were Hepes (pH 7.0 and pH 7.3), Tris (pH 8.2), and acetate (pH 5.0). Fluorescence studies *in vitro* were performed on a BMG Polarstar Galaxy fluorescence plate reader or on a Jasco FP-6500 spectrofluorometer. Absorbance studies were done on an HP 8452a diode array spectrophotometer (Fig. 4B). Reactivity with different thiols was quantified by measuring the increase in fluorescence at 520 nm (490 nm excitation) over time in the plate reader using 5  $\mu\text{M}$  DSSA<sub>Ar</sub> probe and 1.5 mM of the specified thiol reductant (Fig. 5). Total fluorescence change was also

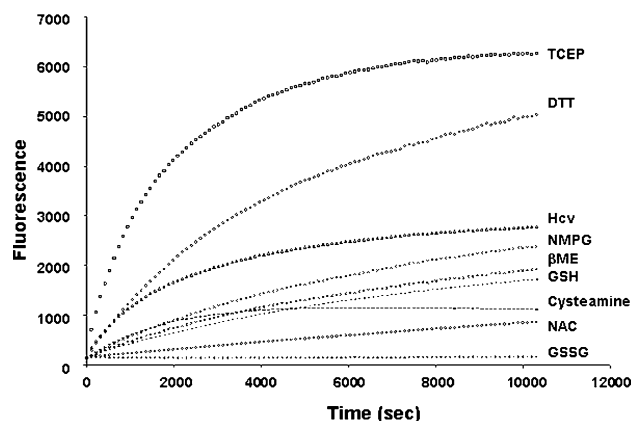


Fig. 5. Reduction of the DSSA<sub>Al</sub> probe by various thiols and TCEP. Reductants always were present at 1.5 mM, and DSSA<sub>Al</sub> was at 5  $\mu\text{M}$  in a Tris buffer (100 mM, pH 8.2) at 25 °C. Reductants used were *N*-acetyl cysteine (NAC), cystamine, reduced glutathione (GSH), 2-mercaptoethanol ( $\beta$ ME), *N*-methyl(2-thiopropionyl)glycine (NMPG), homocysteine (Hcy), dithiothreitol (DTT), and tris(2-carboxyethyl)phosphine hydrochloride (TCEP). Control reaction was with oxidized glutathione (GSSG). Fluorescence readings are averages of five replicates, always with standard deviations less than 5%. Plateau values for the curves are a function of the reduction potential for the reductant, whereas initial rates are a function of the reactivity of the reductant, usually a thiol group. Kinetic measurements were made as in Fig. 4 but now using the BMG Polarstar plate reader.

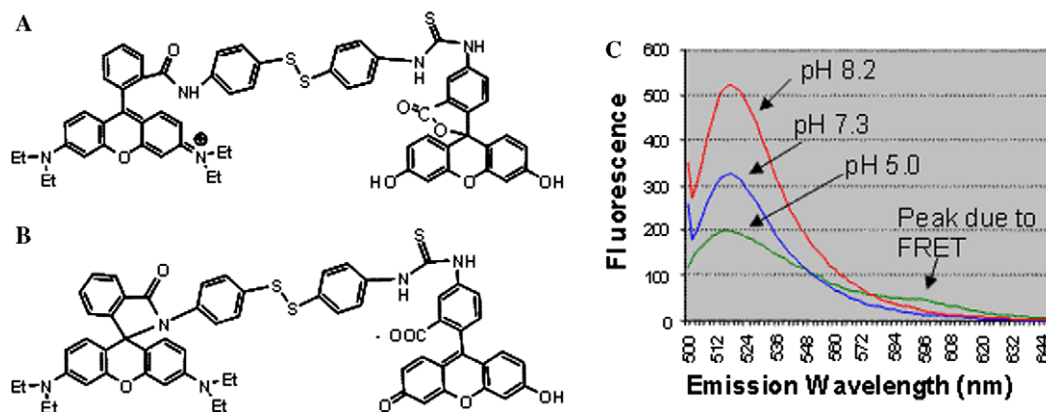


Fig. 3. pH-dependent behavior of the DSSA<sub>Ar</sub> probe [27,28]. The predominant form at low pH (A) is cyclized and neutral at the fluorescein ring, whereas the predominant form at high pH (B) is cyclized and neutral at the rhodamine ring. (C) Fluorescence emission spectra (Ex = 495 nm) of 5  $\mu\text{M}$  DSSA<sub>Ar</sub> at different pH levels. DSSA<sub>Al</sub> (not shown) is identical to DSSA<sub>Ar</sub> except that it has  $-\text{CH}_2-\text{CH}_2-$  linkers in place of the phenyl groups, making it more flexible.

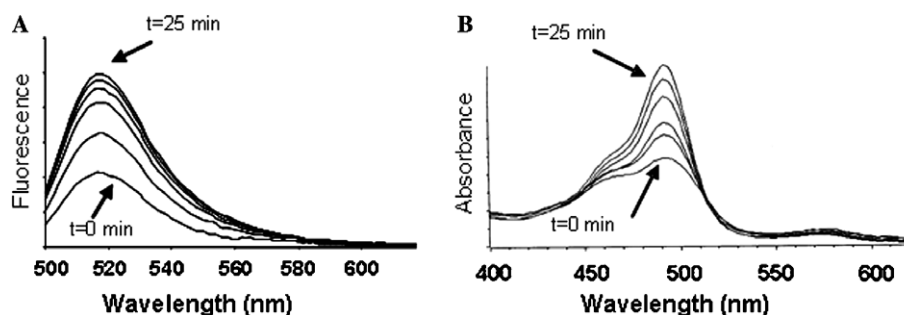


Fig. 4. Spectral changes for 5  $\mu\text{M}$  DSSA<sub>Ar</sub> on exposure to thiol (2.5 mM DTT) at pH 8.2 (100 mM Tris buffer). Spectra were acquired every 5 min and were overlaid. (A) Fluorescence emission (Ex = 495 nm) changes due to reduction. (B) Corresponding absorbance spectra. Similar effects were observed with DSSA<sub>Al</sub>.

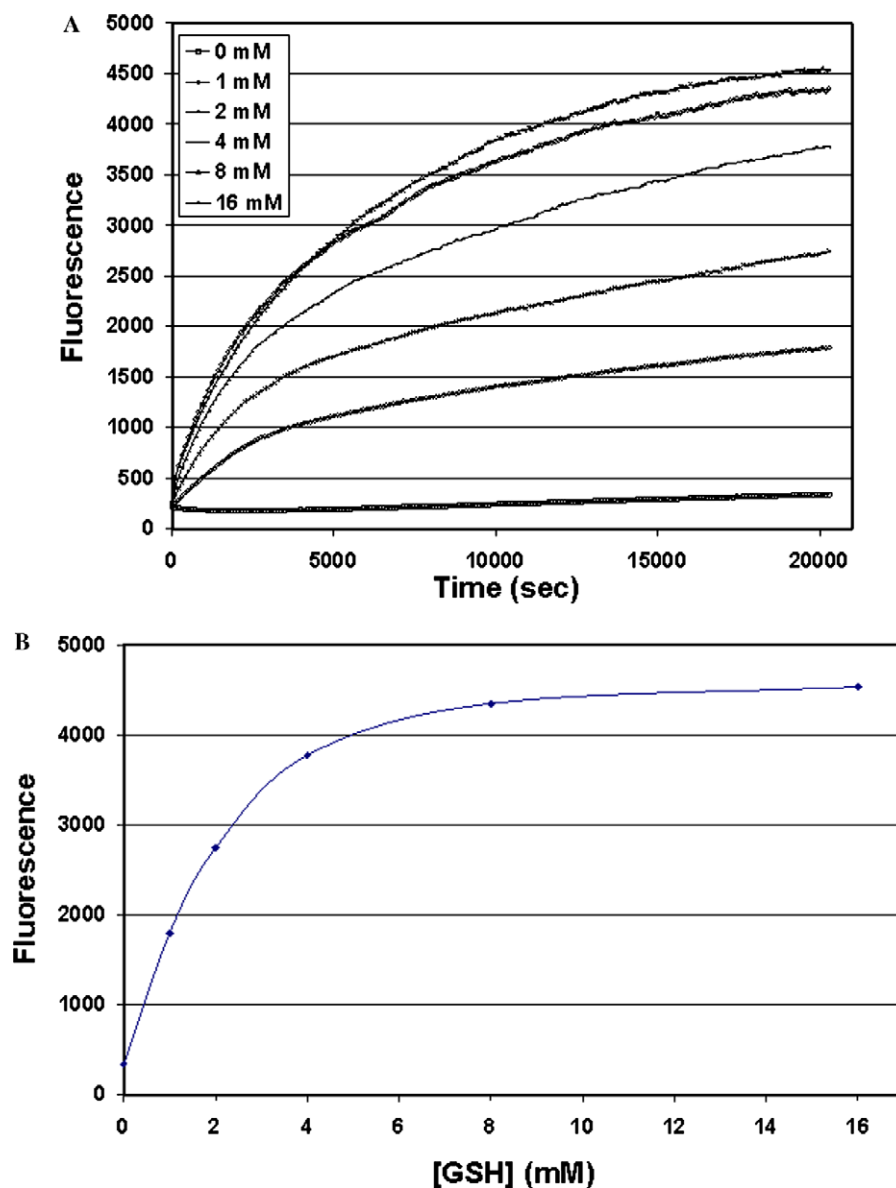


Fig. 6. Reduction of the DSSA<sub>A1</sub> probe as a function of glutathione concentration. (A) Fluorescence increase due to reduction of 5  $\mu$ M DSSA<sub>A1</sub> probe at different concentrations of glutathione in Tris buffer (100 mM, pH 8.2) at 25  $^{\circ}$ C. (B) Plateau values for the reduction reactions in panel A that reflect the equilibrium reached between DSSA<sub>A1</sub> and GSH.

monitored in the plate reader for reduction of 5  $\mu$ M DSSA<sub>A1</sub> at various concentrations of glutathione (Fig. 6).

#### Determination of DSSA reduction potentials

To determine  $E^{\circ}$  values, it was necessary to determine fluorescence for the fully reduced DSSA probes ( $F_{\max}$ ).  $F_{\max}$  could be obtained by titrating 5  $\mu$ M probe with either increasing dithiothreitol (DTT, Fig. 7A) or increasing tris(2-carboxyethyl)phosphine hydrochloride (TCEP, Fig. 7B) at pH 7.0 (100 mM HEPES). Both titrations yielded similar  $F_{\max}$  values, although DTT (and GSH) titrations give atypical kinetics at high concentrations, suggesting some secondary reaction of thiol directly with fluorescein at extremely high thiol concentrations. Therefore, the  $F_{\max}$

value of 9817 obtained from the TCEP titration was used for  $E^{\circ}$  calculations for DSSA<sub>A1</sub>. Equilibrium fluorescence values ( $F_i$ ) were measured at each concentration of DTT reductant, and these data were used along with the  $F_{\max}$  value and the  $E^{\circ}$  of DTT to calculate  $E^{\circ}$  for DSSA<sub>A1</sub> (Table 1). For these reduction measurements, and for the general measurement of thiol levels, the fraction of probe that remains in the oxidized state after equilibration with a reductant (e.g., DTT) is given by

$$X = \frac{[\text{DSSR}]}{([\text{DSSR}] + [\text{DS}])} = \frac{(F_{\max} - F_i)}{(F_{\max} - F_0)}, \quad (1)$$

where  $F_{\max}$  is the fluorescence ( $E_x = 490$  nm,  $E_m = 520$  nm) for fully reduced probe (DS) (Fig. 7),  $F_i$  is

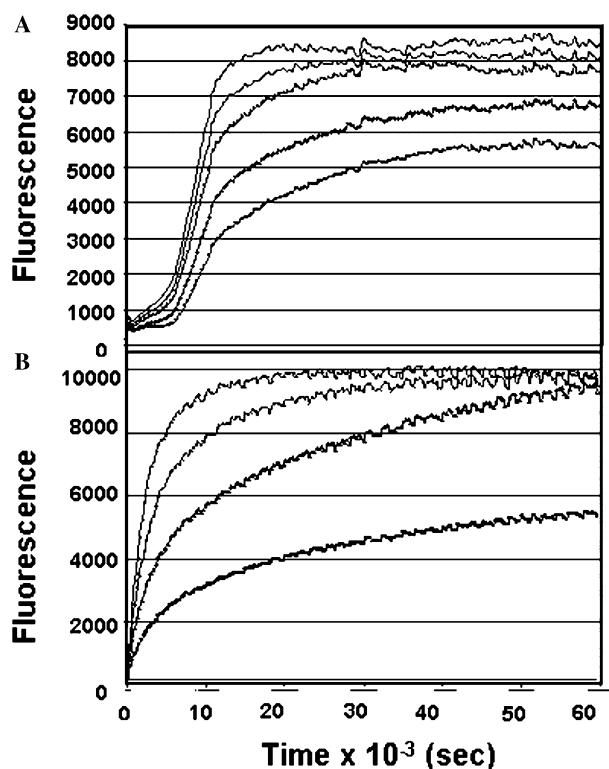


Fig. 7. Fluorescence titrations used to calculate  $E^{\circ}$  for the DSSA<sub>AI</sub> probe. (A) Reduction of 5  $\mu$ M probe by increasing concentrations of DTT (20, 40, 80, 160, and 320 mM) at pH 7.0 in 100 mM Hepes buffer at 25 °C. (B) Reduction of 5  $\mu$ M DSSA<sub>AI</sub> by increasing concentrations of TCEP (11.5, 23, 46, and 92 mM) under the same conditions as in panel A. In the TCEP titration, the same plateau was reached at any concentration greater than 23 mM reductant, whereas with DTT it was not possible to titrate to high enough a concentration to get an accurate estimate of the fluorescence for fully reduced DSSA<sub>AI</sub> because DTT concentrations greater than 320 mM gave atypical kinetics suggestive of reaction other than dithiol reduction.

the fluorescence at some concentration of reductant, and  $F_0$  (=150) is the fluorescence for fully oxidized probe (DSSA). From  $X$ , an equilibrium constant for DSSA reduction can be calculated according to

$$K_{\text{eq}} = \frac{[R_{\text{Ox}}][\text{DS}][\text{AS}]}{[R_{\text{Red}}]^n[\text{DSSA}]}$$

$$= \frac{([\text{DSSA}]_0(1 - X))^3}{[\text{DSSA}]_0(X)([R]_0 - n[\text{DSSA}]_0(1 - X))^n} \quad (2)$$

Table 1  
Calculation of reduction potential for the DSSA<sub>AI</sub> probe

DTT <sub>red</sub>	DSSA $\times 10^6$	DS $\times 10^6$	DTT <sub>ox</sub> $\times 10^6$	$K_{\text{eq}} \times 10^{10}$	$F_i$	$E_{\text{Assay}}$	$E^{\circ}_{\text{DSSA}}^a$
0.02	2.18	2.82	2.82	5.16	5605	-0.275	-0.605
0.04	1.60	3.40	3.40	6.15	6726	-0.273	-0.603
0.08	1.10	3.90	3.90	6.77	7695	-0.271	-0.601
0.16	0.686	4.31	4.31	7.32	8491	-0.270	-0.600
0.04	1.87	3.13	3.13	4.10	6200	-0.278	-0.608
0.08	1.21	3.79	3.79	5.63	7478	-0.274	-0.604
0.16	0.965	4.04	4.04	4.25	7951	-0.277	-0.607

<sup>a</sup>  $E^{\circ}_{\text{DSSA}} = -0.604 \pm 0.003$ .

For a dithiol reductant such as DTT,  $n=1$ . For a monothiol reductant such as GSH,  $n=2$ .  $R$  is reductant,  $[R]_0$  is initial concentration of reductant, and  $[\text{DSSA}]_0$  is initial concentration of probe. From  $K_{\text{eq}}$  and the reduction potential for DTT (-0.33 V [18]), the DSSA reduction potential can be calculated according to

$$E^{\circ}_{\text{DSSA}} = E^{\circ}_{\text{DTT}} + RT/nF \ln(K_{\text{eq}})$$

$$= -0.33 \text{ V} + (0.0592/2) \log(K_{\text{eq}}), \quad (3)$$

where  $R$  is the gas constant,  $T$  is the temperature in Kelvin,  $F$  is Faraday's constant, and  $n$  is the number of electrons transferred. Sample calculations are given in Table 1. Analogous titrations were performed with DSSA<sub>Ar</sub> to obtain its  $E^{\circ}$  value.

#### *E. coli* uptake studies

*Escherichia coli* BL21(DE3)pLysS cells were grown in 10 ml Luria-Bertani (LB) broth overnight and then transferred to 250 ml LB broth and stirred at 37 °C until OD<sub>600</sub> = 0.6 to 0.7 was reached. For dose-response studies (Fig. 8), cells were exposed to various concentrations of DSSA<sub>Ar</sub> probe for 60 min, 1-ml aliquots were taken and centrifuged before being washed with 4  $\times$  1 ml Tris buffer (100 mM, pH 8.2), and fluorescence was read (Ex = 489 nm, Em = 518 nm) on the Jasco spectrofluorometer.

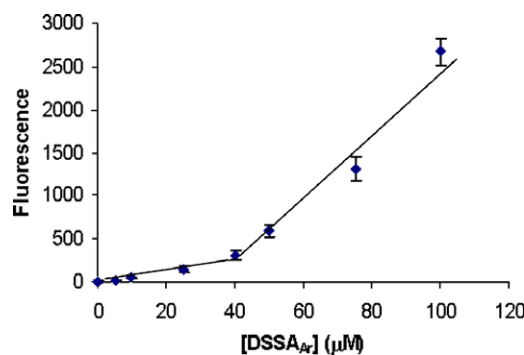


Fig. 8. Dose-response curve for DSSA<sub>Ar</sub> uptake into *E. coli* cells grown in LB media. Five replicate measurements were made at each concentration of probe, with standard deviations indicated as error bars.

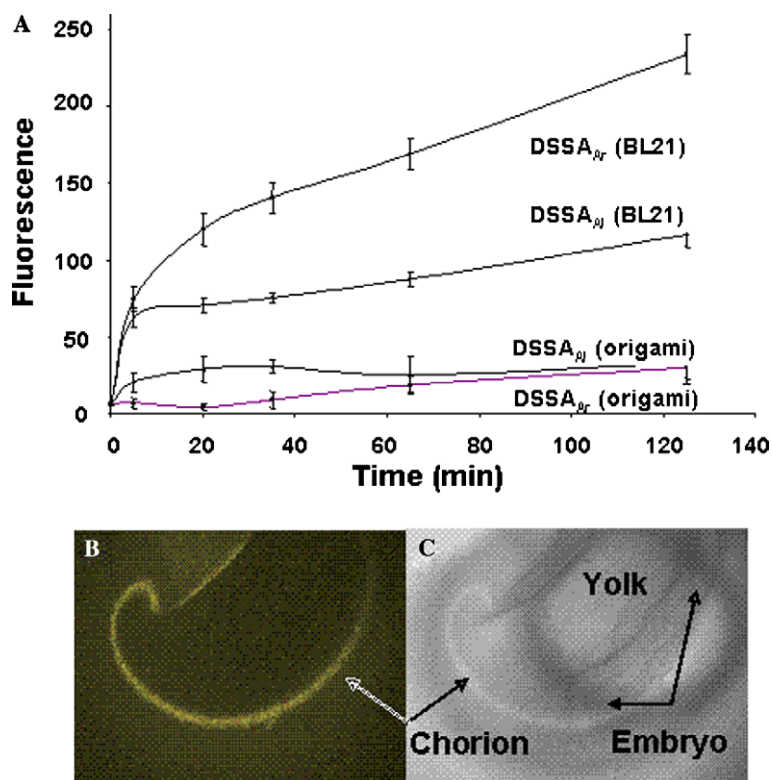


Fig. 9. In vivo detection of thiols with DSSA probes. (A) Uptake into *E. coli*, measured by incubating for various times with 10  $\mu$ M probe, washing cells, and then reading fluorescence for the resuspended cells. (B) Fluorescence image (Ex = 489 nm, Em = 520 nm) of zebrafish embryo at 1 day postfertilization after exposure to 50  $\mu$ M DSSA. (C) Corresponding bright field image. Chorion is equally labeled using probe with aliphatic (DSSA<sub>Al</sub>) or aromatic (DSSA<sub>Ar</sub>) linkers, and whether microinjected or incubated with probe, followed by washing.

For studies of the kinetics of DSSA uptake into *E. coli* BL21 cells (Fig. 9A), the OD<sub>600</sub> = 0.6 to 0.7 culture was partitioned into three equal fractions. One fraction was kept as a blank, and the two DSSA probes (aromatic or aliphatic linker) were added to the other two fractions. In this study, the DSSA probe concentration was 10  $\mu$ M, and the carrier dimethyl sulfoxide (DMSO) was kept at less than 0.5%. The cell culture was stirred for 2 h, and 1-ml samples were collected at 0-, 15-, 30-, 60-, and 120-min intervals. The samples were centrifuged for 5 min at 13,000 rpm, and the supernatant was decanted. The cell pellet was resuspended in 1 ml Tris buffer (100 mM, pH 8.2), vortexed for 5 s, and centrifuged for 5 min at 13,000 rpm before the supernatant was decanted. This washing was done three times to ensure complete removal of any DSSA probe bound on the surface of the cells. Finally, just before the fluorescence reading, the pelleted cells were resuspended in Tris buffer (100 mM, pH 8.2) and fluorescence from the suspended cells was recorded. On average, the time between cell pelleting and fluorescence reading was kept constant at 2 h. All of the results presented in this study are the averages of five replicates with standard deviations less than 10%. Appropriate blanks with cultured cells were used to minimize error from light scattering. This whole process was repeated with Origami cells, with the standard deviations for these replicates also being less than 10%.

#### Zebrafish studies

Zebrafish embryos were grown and maintained at the Marine and Freshwater Biomedical Sciences Center at UW-Milwaukee using standard protocols [19] in accordance with accepted procedures of humane animal care. At 1 day postfertilization, embryos were exposed externally to 50  $\mu$ M DSSA probe for 1.5 h or probe was microinjected past the chorion. Embryos were then washed and immobilized in methylcellulose. Injections and incubations were done with 50  $\mu$ M DSSA in 1% DMSO in Danieau's buffer (58 mM NaCl, 0.7 mM KCl, 0.4 mM MgSO<sub>4</sub>, 0.6 mM Ca(NO<sub>3</sub>)<sub>2</sub>, 0.5 mM Hepes, pH 7.6). Fluorescence images were obtained with an Olympus IX70 microscope (Ex = 489 nm). Images were processed using MetaMorph software (Molecular Devices).

#### Results and discussion

##### Synthesis and in vitro reactivity of the DSSA probes

As an initial donor/acceptor (D/A) pair, fluorescein/rhodamine (others such as coumarin/fluorescein are possible as well) was attached to diaminophenyl disulfide to create the DSSA<sub>Ar</sub> probe (Fig. 1). The corresponding probe with an aliphatic linker (DSSA<sub>Al</sub>) was prepared using cystamine (Fig. 2B). An important property of

both fluorophores in the DSSA reagents is that they are capable of cyclization reactions, such that they can exist in different forms that interconvert in a pH-dependent fashion (Fig. 3). The observation of some fluorescence resonance energy transfer (FRET) at pH 5.0 ( $E_x = 495$ ,  $E_m = 520$  nm) indicates that there is opening of the cyclic lactam on the rhodamine ring, permitting energy transfer from the fluorescein that remains ring-opened to the now fluorescent rhodamine. Lack of FRET at pH 7.3 indicates that the rhodamine ring is fully in the neutral form. The decrease in fluorescence from fluorescein in going from pH 8.2 to pH 7.3 indicates that the fluorescein is approximately 50% in the neutral and cyclized form at pH 7.3. These data demonstrate that the DSSA probe containing fluorescein and rhodamine populate ring-open and ring-closed forms for both fluorophores in a pH-dependent fashion, a requirement for such a probe to be both fluorescent and able to cross cell walls. Furthermore, the probe should remain fluorescent over a wide pH range, as was demonstrated for the Adamczyk and Grote probe that had fluorescein and rhodamine permanently tethered [11]. Although the pH-dependent cyclizations could be prevented by using halogenated or other analogs of these fluorophores [20–22], this behavior was viewed as a desirable feature of the DSSA probes because equilibration with ring-closed forms permits transient formation of a neutral species that is able to penetrate hydrophobic cell walls. As can be seen, reduction of the dithiol yields an increase in fluorescence for fluorescein due to removal of quenching (Fig. 4A). Surprisingly, there is also an increase in absorbance that occurs on reduction (Fig. 4B), meaning that the DSSA probe can be used to detect thiols based on changes in either absorbance or emission by fluorescein (DS). The reason for the dramatic change in the absorbance spectrum is not clear given that reduction of the dithiol linker would not be expected to affect fluorescein's electronic state. But there clearly must be some chemical interaction between the fluorescein and rhodamine fluorophores that most likely stack through hydrophobic interactions.

The DSSA probes react in a concentration-dependent manner with various thiols as well as TCEP, the recently developed reagent for reducing dithiols [23]. Relative reaction rates with both DSSA<sub>AI</sub> and DSSA<sub>Ar</sub> at pH 8.2 are as follows: TCEP > DTT, homocysteine > GSH,  $\beta$ -mercaptoethanol (Fig. 5). Besides variability in rate of reaction, the fluorescence endpoint varies significantly, a function of reduction potential for each reductant. These data highlight an especially useful property of the DSSA probes, namely that a small amount of probe (5  $\mu$ M) yields significant changes in fluorescence for even a relatively strong reductant (DTT  $E^{\circ} = -0.33$  V), but only at very high reductant concentrations (>1 mM). This effect is demonstrated for glutathione in its physiologically relevant concentration range of 1 to 10 mM. At the low concentrations of probe (5  $\mu$ M) that might be present

inside a cell, there are significant changes in fluorescence as glutathione increases from 1 to 10 mM (Fig. 6). Because only 5  $\mu$ M probe is present (an insignificant amount compared with cellular glutathione levels of 1–10 mM), the probe will not affect the intracellular redox state. This behavior of the DSSA probe is a result of its unusually low reduction potential.

#### Reduction potential for the DSSA probes

Reduction potentials for the probes were calculated by equilibrating with DTT or TCEP and calculating an equilibrium constant based on fluorescence changes for fluorescein (Fig. 7). Potentials were calculated at pH 7.0 from the Nernst equation, using  $E^{\circ} = -0.33$  V for DTT [18] and  $E^{\circ} = -0.29$  V for TCEP (unpublished results). The reduction potentials are surprisingly low for both DSSA<sub>Ar</sub> ( $E^{\circ} = -0.66 \pm 0.03$  V) and DSSA<sub>AI</sub> ( $E^{\circ} = -0.604 \pm 0.002$ ), again suggesting that their use in vivo will not disrupt the intracellular redox state by oxidizing the cell. It also means that approximately 10  $\mu$ M of the DSSA probe will not oxidize proteins if it is used to measure thiols produced in a continuous coupled enzyme assay, where protein is typically present at less than 100 nM. The main restriction on using the DSSA probes for in vitro continuous enzyme assays is that the thiol being monitored should be present at high enough concentrations (>0.2 mM) to reduce the probe to a detectable level. The thermodynamic difficulty in reducing the DSSA probes may be related to the presence of stabilizing chemical interactions between fluorophores, as discussed above in association with the results of Fig. 4B. But it is a useful property in that it avoids the undesired oxidation of cellular thiols in vivo and of high- $K_m$  proteins being assayed in vitro.

#### Detection of thiols in vivo using the DSSA probes: *E. coli* and zebrafish

In addition to measuring thiol levels in vitro, the DSSA probes can be used to detect thiols in vivo. Specifically, incubation of *E. coli* cells with either form of the probe showed a concentration-dependent (Fig. 8) and time-dependent (Fig. 9A) uptake into cells. Analogous uptake studies in *E. coli* Origami cells [17], which are not able to synthesize glutathione, show much less fluorescence signal. Therefore, fluorescence intensity must reflect levels of reduced thiols in the bacteria. Interestingly, there seems to be more uptake and reduction with the aromatic linker version of the probe (DSSA<sub>Ar</sub>). This demonstrates the importance of comparing the two linker classes for in vivo studies.

As a complement to these bacterial uptake studies, the DSSA probes were used to monitor thiol levels in zebrafish embryos. At 1 day postfertilization, either embryos were incubated with probe (1 h) or probe was microinjected past the chorion. In both cases, significant accumulation of probe was observed in the chorion

(Fig. 5B), suggesting the presence of thiol-rich proteins in the chorion. High-cysteine content proteins have been reported in the chorion of *Bombyx mori*, with a proposed role in protecting the developing embryo from environmental insults [24]. Although such thiol-rich proteins have not yet been reported in the chorion of teleosts such as zebrafish, the results reported here suggest that they may be present. Functional proteomic work in our laboratory is being directed toward defining such proteins in the fish chorion as well. More broadly, DSSA probes should have utility for histological staining of thiol-rich tissue samples and the staining of thiols in subcellular compartments. Because the dithiol of DSSA is highly selective for thiols, these probes have advantages over fluorophores tethered to less selective electrophiles such as maleimide, alkyl halides, and iodoacetamide [5,25,26].

## Conclusions

DSSA probes composed of fluorescein tethered to rhodamine via a disulfide linkage can be prepared as single isomers with high purity. These reagents are able to detect and label thiols in vivo because they can exist in a neutral form that is able to penetrate cell walls. The reagents can be used to label cellular thiols with fluorophores that permit imaging over a wide pH range [11]. They can also be used in a continuous thiol assay, whereby an increase in fluorescence from fluorescein is monitored as the disulfide bond is reduced. The low reduction potential ( $E^{\circ} = -0.6\text{ V}$ ) of the DSSA probes means that they (i) will not cause oxidative stress to cells and (ii) can be present at low concentrations (5  $\mu\text{M}$ ) and still be responsive to changes in thiol levels in the physiologically relevant range of 1 to 10 mM.

## Acknowledgments

We thank Mark Steinmetz for providing helpful discussions, Ron Raines for suggesting the use of Origami cells, and the NIEHS Marine and Freshwater Biomedical Sciences Center (NIH Grant ES-04184) for allowing the use of its facility. This work was supported in part by grants from the American Heart Association (0530307Z) to Daniel Sem and from the Department of Defense (W81XWH-05-1-0476) to Phani Pallela.

## References

- [1] I. Rahman, W. MacNee, Regulation of reduction glutathione levels and gene transcription in lung inflammation: therapeutic approaches, *Free Radic. Biol. Med.* 28 (2000) 1405–1420.
- [2] C. Hwang, A.J. Sinskey, H.F. Lodish, Oxidized reduction state of glutathione in the endoplasmic reticulum, *Science* 257 (1992) 1496–1502.
- [3] K.J. Davies, Oxidative stress: the paradox of aerobic life, *Biochem. Soc. Symp.* 61 (1995) 1–31.
- [4] G.L. Ellman, Tissue sulfhydryl groups, *Arch. Biochem. Biophys.* 82 (1959) 70–78.
- [5] R.P. Haugland (Ed.), Handbook of fluorescent probes and research chemicals, ninth ed., Molecular Probes, Eugene, OR, 2002.
- [6] F. Hochgrafe, J. Mostertz, D. Albrecht, M. Hecker, Fluorescence thiol modification assay: oxidatively modified proteins in *Bacillus subtilis*, *Mol. Microbiol.* 58 (2005) 409–425.
- [7] K. Tyagarajan, E. Pretzer, J.E. Wiktorowicz, Thiol-reactive dyes for fluorescence labeling of proteomic samples, *Electrophoresis* 24 (2003) 2348–2358.
- [8] M.E. Kosower, S.N. Kosower, Bromobimane probes for thiols, *Methods Enzymol.* 251 (1995) 133–148.
- [9] S.J. Kim, T.R. Raines, Dibromobimane as a fluorescent crosslinking reagent, *Anal. Biochem.* 225 (1995) 174–176.
- [10] C.T. Dooley, T.M. Dore, G.T. Hanson, W.C. Jackson, S.J. Remington, R.Y. Tsieng, Imaging dynamic redox changes in mammalian cells with green fluorescent protein indicators, *J. Biol. Chem.* 279 (2004) 22284–22293.
- [11] M. Adamczyk, J. Grote, Synthesis of probes with broad pH range fluorescence, *Bioorg. Med. Chem. Lett.* 13 (2003) 2327–2330.
- [12] M. Mandala, G. Serck-Hanssen, G. Martino, K.B. Helle, The fluorescent cationic dye rhodamine 6G as a probe for membrane potential in bovine aortic endothelial cells, *Anal. Biochem.* 274 (1999) 1–6.
- [13] R.P. Haugland (Ed.), Handbook of fluorescent probes and research chemicals, sixth ed., Molecular Probes, Eugene OR, 1996.
- [14] M. Adamczyk, J. Grote, Efficient synthesis of rhodamine conjugates through the 2'-position, *Bioorg. Med. Chem. Lett.* 10 (2000) 1539–1541.
- [15] A.P. Senft, T.P. Dalton, H.G. Shertzer, Determining glutathione and glutathione disulfide using the fluorescent probe *o*-phthalaldehyde, *Anal. Biochem.* 280 (2000) 80–86.
- [16] S. Liu, N.H. Ansari, C. Wang, L. Wang, S.K. Srivastava, A rapid HPLC method for the quantification of GSH and GSSG in ocular lens, *Curr. Eye Res.* 15 (1996) 726–732.
- [17] A.I. Derman, W.A. Prinz, D. Belin, J. Beckwith, Mutations that allow disulfide bond formation in the cytoplasm of *Escherichia coli*, *Science* 262 (1993) 1744–1747.
- [18] W.W. Cleland, Dithiothreitol, a new protective reagent for SH groups, *Biochemistry* 3 (1964) 480–485.
- [19] M. Westerfield, *The Zebrafish Book: A Guide for the Laboratory Use of Zebrafish (Danio rerio)*, fourth ed., University of Oregon Press, Eugene, 2000.
- [20] K.R. Gee, M. Poot, D.H. Klaubert, W.-C. Sun, R.P. Haugland, F. Mao, Fluorinated xanthene derivatives, US patent. 6 (162), (2000) 931.
- [21] T. Nguyen, M.B. Francis, Practical route to functionalized rhodamine dyes, *Org. Lett.* 5 (2003) 3245–3248.
- [22] Y. Urano, M. Kamiya, K. Kanda, T. Ueno, K. Hirose, T. Nagano, Evolution of fluorescein as a platform for finely tunable fluorescence probes, *J. Am. Chem. Soc.* 127 (2005) 4888–4894.
- [23] E.B. Getz, M. Xiao, T. Chakrabarty, R. Cooke, P.R. Selvin, A comparison between the sulfhydryl reductants tris(2-carboxyethyl)phosphine and dithiothreitol for use in protein biochemistry, *Anal. Biochem.* 273 (1999) 73–80.
- [24] G.C. Rodakis, F.C. Kafatos, Origin of evolutionary novelty in proteins: how a high-cysteine chorion protein has evolved, *Proc. Natl. Acad. Sci. USA* 79 (1982) 3552–3555.
- [25] T.O. Sippel, New fluorochromes for thiols: maleimide and iodoacetamide derivatives of a 3-phenylcoumarin fluorophore, *J. Hist. Cytochem.* 29 (1981) 314–316.
- [26] K. Tyagarajan, E. Pretzer, J. Wiktorowicz, Thiol-reactive dyes for fluorescence labeling of proteomic samples, *Electrophoresis* 24 (2003) 2348–2358.
- [27] H. Takakusa, K. Kikuchi, Y. Urano, H. Kojima, T. Nagano, A novel design method of ratiometric fluorescent probes based on fluorescence resonance energy transfer switching by spectral overlap integral, *Chem. Eur. J.* 9 (2003) 1479–1485.
- [28] M. Matsui, T. Higeta, M. Kimura, K. Funabiki, K. Nakaya, Chiral fluorescent labeling reagent derived from rhodamine B for flurbiprofen, *Bull. Chem. Soc. Jpn.* 76 (2003) 1405–1408.

## **Program/Abstract # 86.2**

### **Effect of thiol reductants on estrogen and estrogen receptor: revisiting previous assays**

Phani Kumar Pullela, Kevin Alby, Hector Varela, Daniel S Sem. CPFM, Marquette University, 535 N.14th street, Milwaukee, WI, 53233

The disulfide bridges in proteins play an essential role in maintaining protein structural integrity, function and dynamics. It is common to use thiol reductants like DTT (dithiothreitol) and BME (2-mercapto ethanol) to prevent air oxidation of cysteine residues. Though extensive studies were done over the past forty years, using thiol reductants in protein biochemistry, our recent findings have provided a surprising observation while using these reductants in the estrone-estrogen receptor system. Both BME and DTT were shown to react with estrone in dichloromethane/HCl and the thiohemiketals produced are reasonably stable. Even in the buffered aqueous medium at pH 7.4, the thiohemiketals are stable, making them relevant in protein biochemical studies. We choose, estrogen receptor as model system, due to its importance in breast cancer research and endocrine disruptors. ER-LBD was expressed in E.coli and the protein was obtained in its active conformation by adding estrone during the protein expression. The effect of different thiol reductants was studied by incubating the thiol and protein for three hours. The thiol interaction with estrogen in the binding site is possibly mediated by the His 524 or entropy driven due to large volume of ER-LBD binding site. The possible reaction of thiol reductants with the ketone of D-ring on estrone raises concerns for their use in relevant protein biochemistry. This work is being funded by the US Army Medical Research and Materiel Command's "Breast Cancer Research Program (BCRP) # BC046402.

# A Dithio-Coupled Kinase and ATPase Assay

TAURAI CHIKU, PHANI KUMAR PULLELA, and DANIEL S. SEM

Kinases and ATPases produce adenosine diphosphate (ADP) as a common product, so an assay that detects ADP would provide a universal means for activity-based screening of enzymes in these families. Because it is known that most kinases accept ATP $\beta$ S (sulfur on the  $\beta$ -phosphorous) as a substrate in place of adenosine triphosphate (ATP), the authors have developed a continuous assay using this substrate, with detection of the ADP $\beta$ S product using dithio reagents. Such an assay is possible because dithio groups react selectively with ADP $\beta$ S and not with ATP $\beta$ S. Thiol detection was done using both Ellman's reagent (DTNB) and a recently developed fluorescent dithio reagent, DSSA. Therefore, the assay can be run in both absorbance and fluorescence detection modes. The assay was used to perform steady-state kinetic analyses of both hexokinase and myosin ATPase. It was also used to demonstrate the diastereoselectivity of hexokinase (R) and myosin ATPase (S) for the isomers of ATP $\beta$ S, consistent with previous results. When run in fluorescence mode using a plate reader, an average  $Z'$  value of 0.54 was obtained, suggesting the assay is appropriate for high-throughput screening. (*Journal of Biomolecular Screening* 2006:1-10)

**Key words:** kinase, dithio, high throughput, continuous assay, chemical proteomic, DSSA

## INTRODUCTION

**K**INASES CATALYZE THE TRANSFER of the  $\gamma$  phosphate of adenosine triphosphate (ATP) to a substrate. They can phosphorylate either "small molecules" or proteins, playing important roles in metabolism and regulation, respectively. A conserved aspartate in the active site acts as a general base, which deprotonates the substrate nucleophile that attacks the  $\gamma$  phosphate.<sup>1</sup> Small-molecule kinases phosphorylate nonprotein substrates such as glucose, pyruvate, and other metabolites. Typically, the coupling of phosphorylation to metabolic reactions transforms thermodynamically unfavorable reactions into highly exergonic reactions. Furthermore, phosphorylation acts as a trapping mechanism to retain metabolites within the cell. Most of the protein kinases are known to phosphorylate serine, threonine, tyrosine, or histidine residues on their substrates. Regulatory proteins and enzymes of various biochemical processes are either activated or deactivated by this phosphorylation. As such, protein kinases play crucial roles in transcription and translation initiation, apoptosis, replication, and many

cell signaling cascades. Indeed, it is estimated that the vertebrate genome has more than 500 protein kinases performing these various functions<sup>2</sup>—so functional proteomic studies of kinases will likely identify many new drug targets, as well as produce a better understanding of the biochemistry behind cellular regulation.

With the sequencing of the human genome and the subsequent race to decode all the genes and their respective functions, the current interest in kinases will undoubtedly continue to grow. They have been linked to disorders such as inflammation and various cancers, making them attractive drug targets. There has already been a heavy investment by the pharmaceutical industry in drugs that target protein kinases,<sup>3</sup> spurred in part by the recent success of Gleevec, which targets Bcr-Abl kinase for the treatment of chronic myelogenous leukemia.<sup>4</sup> Now, more than 40 protein kinase inhibitors are in clinical trials, and many more are in preclinical studies.

This tremendous interest in kinases, both as drug targets and as targets of functional genomic/proteomic studies, means there is a need for more efficient and general high-throughput assays. Although displacement assays have been developed for kinases,<sup>5,6</sup> activity-based assays are advantageous because they are more sensitive and direct, detecting changes in the biochemical activity associated with the biological function of the enzyme. At a minimum, it will always be important to complement a displacement-based assay with an activity-based assay. Although some widely used activity-based assays monitor phosphorylation of a peptide product using antibodies,<sup>7-9</sup> the

Chemical Proteomics Facility at Marquette, Department of Chemistry, Marquette University, Milwaukee, WI.

Received Nov 25, 2005, and in revised form Jun 16, 2006. Accepted for publication Jun 21, 2006.

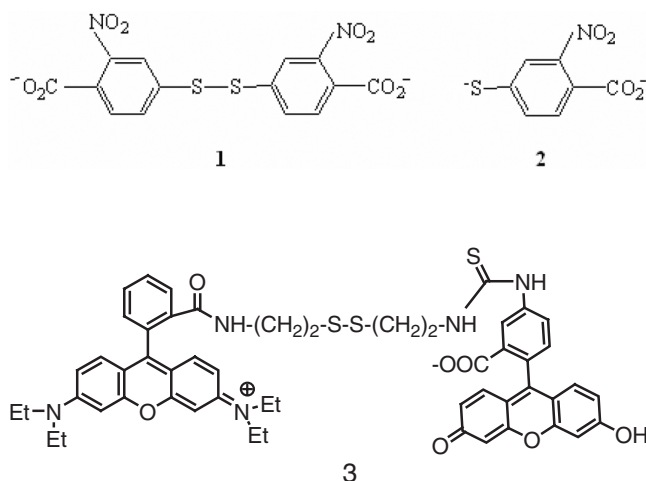
*Journal of Biomolecular Screening* 11(X); 2006  
DOI:10.1177/1087057106292142

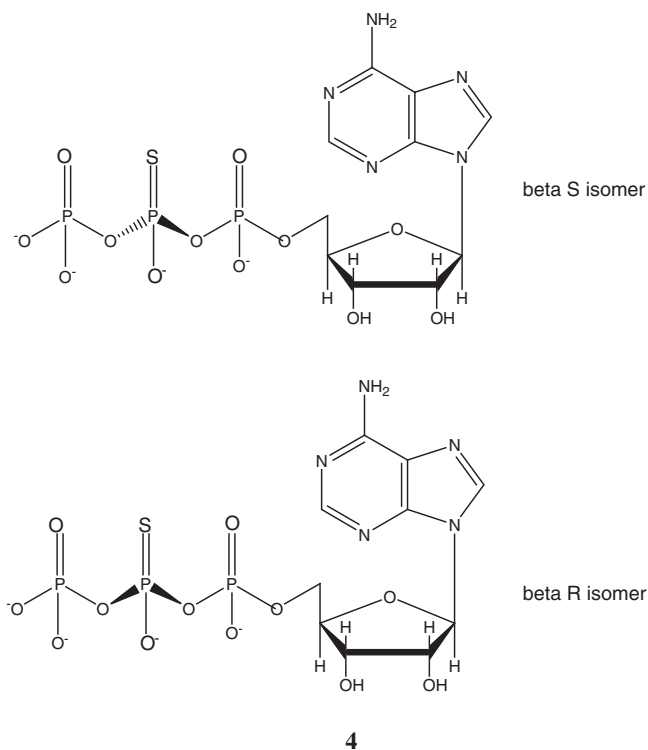
most general activity-based assays are those that monitor the ATP to adenosine diphosphate (ADP) conversion, which is common to all kinases irrespective of which substrate it phosphorylates. There are many kinase assays available, including scintillation proximity assay (SPA)-based, fluorescence polarization (FP)-based, and fluorescence resonance energy transfer (FRET)-based assays.<sup>10</sup> One widely used assay is IMAP (Molecular Devices, Sunnyvale, CA), which is a fluorescence polarization assay where phosphorylated peptide is captured on a metal-derivatized nanoparticle.<sup>11</sup> Another commonly used assay strategy is to monitor production of a phosphorylated peptide in an FP assay, based on displacement of a fluorescently tagged phosphor-peptide from an antibody.<sup>5</sup> Such assays have been developed for both tyrosine and serine/threonine kinases.<sup>12</sup> A clever variation of this antibody displacement assay is the Transcreener™ assay (BellBrook Labs, Madison, WI), where fluorescently tagged ADP is displaced from antibodies raised against ADP. This assay has the potential to be a universal kinase assay, if adequate antibody selectivity for ADP over ATP can be achieved. But any antibody displacement assay is limited by the specificity of the antibody and may be prone to false positives from compounds that bind to the antibody. It is also possible to monitor ATP levels with a recently reported luminescent assay,<sup>13,14</sup> which shows a decreasing signal as ATP is consumed. An assay that detects ADP production and gives an increasing fluorescence signal over time is currently not available, to our knowledge.

A more traditional kinase assay is a “coupled assay,” which detects the production of ADP using a pyruvate kinase (PK)/lactate dehydrogenase (LDH) assay. In this PK/LDH-coupled assay, ADP is phosphorylated by phosphoenol-pyruvate, catalyzed by PK. The pyruvate produced in this reaction is then reduced by nicotinamide adenine dinucleotide (NADH), catalyzed by LDH. One then monitors the disappearance of NADH, which has an extinction coefficient of  $\epsilon_{340\text{ nm}} = 6.22\text{ mM}^{-1}\text{cm}^{-1}$ . Three major drawbacks of such an approach are apparent: (1) monitoring decreasing levels of NADH puts a rigid restriction on the dynamic range of the assay because too large an excess of NADH would give an absorbance outside the linear range, (2) the need to use coupling enzymes adds more reaction steps and therefore more work to validate the assay and verify hits, and (3) sensitivity is limited by the relatively low extinction coefficient of NADH. Herein we propose an alternative continuous assay that overcomes these limitations and can be used in either absorbance- or fluorescence-based detection modes. A survey of recent advances in enzyme screening shows a preference for chromogenic<sup>15-17</sup> assays using high molar absorptivity dyes, as well as fluorogenic<sup>18-21</sup> assays. Most of these systems involve direct measurements or coupling to another chemical reaction, which simplifies the assay. Protein kinase assays based on fluorophores are being developed,<sup>7,22,23</sup> with many used in

high-throughput screening (HTS)<sup>24-26</sup> applications. These assays are based on substrate displacement or substrate turnover (with direct or indirect detection). The latter is especially desirable because it provides signal amplification, permitting detection of enzyme at low concentrations.

- Clearly, there is a need for an inexpensive, simple, sensitive, universal, and continuous activity-based assay that monitors an increasing signal. This assay should be amenable to HTS as well as functional proteomic studies to address the growing interest in kinases in drug discovery and basic cell biology. We therefore developed a general kinase assay based on the use of a well-tolerated ATP analogue, which yields a corresponding dithio-reactive ADP analogue during the kinase reaction. It has been demonstrated that there is differential reactivity of ATP $\beta$ S and ADP $\beta$ S<sup>27</sup> (thiol analogues of ATP and ADP, respectively) toward dithio groups. Furthermore, the presence of the sulfur atom introduces chirality on the  $\beta$  phosphorus. It has been demonstrated that kinases will prefer one diastereomer over the other (R/S) as a substrate. This stereochemical preference has not been extensively explored in protein kinases due to the difficulty of performing such studies for nonenzymologists, although the preference is well documented for a number of small-molecule kinases.<sup>27</sup> To demonstrate the ease of determining diastereotopic preference using the dithio-coupled assay, studies were done herein with representative enzymes in each diastereotopic class: those that prefer the R (hexokinase) or S (myosin) ATP $\beta$ S diastereomers. In our studies, a dithio-bridged chromophore or fluorophore was used for detection. The chromogenic assay uses *bis*-dithionitrobenzoic acid (DTNB = Ellman's reagent) (**1**), which is known to yield a yellow-colored chromophore (**2**) ( $\beta_{412\text{ nm}} = 13.5\text{ mM}^{-1}\text{cm}^{-1}$ ) after cleavage.<sup>28</sup> The fluorogenic assay uses a recently developed dithio probe (DSSA), consisting of a cystamine linker and substituted with rhodamine and fluorescein (**3**).<sup>29</sup>





- This assay avoids the drawbacks associated with the traditional NADH-based coupled assay in the following ways: (1) the more than 2-fold increase in molar extinction coefficient leads to an enhancement in sensitivity, (2) measurement of an increasing signal permits improvement in the dynamic range of the assay, and (3) there is no need for coupling to an enzyme reaction, which simplifies assay validation and hit verification procedures. The assay also provides structural information about the ATP binding site, in terms of diastereotopic preference for the R or S form of ATP $\beta$ S, if this information is desired. Finally, it can be performed using either absorbance- or fluorescence-based detection modes.

## MATERIALS AND METHODS

### Instrumentation and data processing

A Pharmacia fast protein liquid chromatography (FPLC) system, model LCC-501, was used for purifying ATP $\beta$ S from the enzymatic synthesis mixture. An HP 8452A diode array spectrophotometer was used for analysis of column fractions, as well as for the UV/Vis-based kinase assay measurements. All spectroscopic measurements were taken at 25 °C in a 1-mL quartz cuvette. Time course measurements were at 4-sec intervals for at least 15 min. Steady-state kinetic data were fitted to the Michaelis-Menton or sigmoidal dose-response ( $IC_{50}$ ) equations using the nonlinear least squares fitting algorithm in

SigmaPlot 8.0. Fluorescence measurements were made on a BMG Polarstar plate reader at 25 °C, using 96-well plates. The reader was equipped with 485-nm excitation and 520-nm emission filters, both with a 10-nm bandpass.  $^{31}P$  NMR spectra were acquired on a 300-MHz ( $^1H$ ) Varian nuclear magnetic resonance (NMR) spectrophotometer at room temperature and approximately pH 10, using  $H_3PO_4$  as reference. Processing was done using the NUTS<sup>®</sup> software package.

### Materials

All salts, buffers, and enzymes, except where noted, were from Sigma-Aldrich (St. Louis, MO) and were of biochemical reagent grade. They were used without any further treatment or purification. Buffer pH was adjusted using either NaOH or HCl. Sephadex DEAE A25<sup>®</sup> resin and packed columns were from Amersham Biosciences (Piscataway, NJ). The resin was prepared for use according to the supplier's procedure. Polyethyleneimine-cellulose thin-layer chromatography (TLC) plates were from VWR (West Chester, PA). Triethylamine was used to prepare triethylammonium bicarbonate buffer by bubbling carbon dioxide gas into a 2-M solution of triethylamine until the pH was between 7.6 and 7.8. The exact concentration of the buffer was determined by a back titration after addition of excess HCl. Enzymes were from the following organisms: LDH (rabbit muscle), PK (rabbit muscle), acetate kinase (*Escherichia coli*), myosin (pig), hexokinase (*Saccharomyces cerevisiae*), and glucose-6-phosphate dehydrogenase (G6PDH; *Leuconostoc mesenteroides*).

### Synthesis of ATP $\beta$ S: the R diastereomer<sup>27</sup>

The following reaction mixture (total volume 7.0 mL) was prepared: 3.6 mM ADP $\beta$ S, 7.2 mM  $MgCl_2$ , 72 mM Tris-HCl (pH 8.0), 0.55 mM dithiothreitol, and 28.5 mM acetate phosphate. The, 500 U of acetate kinase was added, and progress of the reaction was followed by spotting the mixture on PEI-cellulose TLC plates at 30-min intervals, using pH 3.5  $KH_2PO_4$  as the solvent. The reaction was almost complete after 6 h. ATP $\beta$ S was purified from the mixture using a Sephadex DEAE A25<sup>®</sup> gravity or FPLC column, with triethylammonium bicarbonate as the mobile phase. A linear gradient of 0.05 M to about 0.5 M buffer was used. The volatile buffer was removed with a rotary evaporator, and any remaining triethylamine was removed by performing at least 2 evaporations in methanol. The solid ATP $\beta$ S (R) product (4) was recovered after freeze drying. The formation of ATP $\beta$ S was confirmed by  $^{31}P$  NMR (Fig. 1A).

### Synthesis of ATP $\beta$ S: the S diastereomer<sup>27</sup>

The following reaction mixture (total volume 17.2 mL) was prepared at 22 °C: 1.36 mM ADP $\beta$ S, 3.65 mM  $MgCl_2$ , 0.85 mM

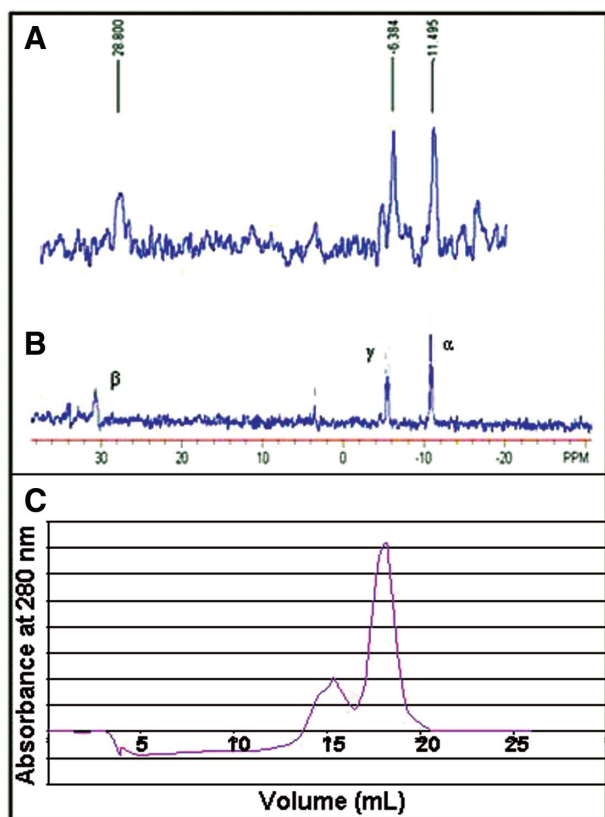


**FIG. 1.** Purity of ATP $\beta$ S.  $^{31}\text{P}$ -NMR spectra<sup>34</sup> of the (A) R diastereomer of ATP $\beta$ S and (B) S diastereomer of ATP $\beta$ S. (C) Elution profile for a typical ATP $\beta$ S purification, showing elution of ADP $\beta$ S followed by ATP $\beta$ S. Detection was at 280 nm.

dithiothreitol, 380 mM KCl, 38 mM Tris-HCl (pH 8.0), 2.0 mM phosphoenolpyruvate, 2.4 mM NADH, and 200 U LDH. Then, 100 U PK was added, and the reaction was followed at 340 nm to monitor consumption of NADH. The reaction was complete in about 3 h, and the ATP $\beta$ S (S) (4) was purified and characterized as described above (Fig. 1B). For both diastereomers, reasonably good chromatographic separation of ATP $\beta$ S and ADP $\beta$ S could be achieved during purification (Fig. 1C).

#### pH stability of DTNB

pH variation studies of the stability of DTNB were done at 25.0 °C with 10 mM DTNB. The following 100-mM buffers were used for preparation of DTNB solutions at pHs close to their respective  $\text{pK}_a$  values: phosphate (3.5), acetate (3.5), HEPES (7.0), Tris-HCl (8.2), and bicarbonate. Then, 10-mM solutions of DTNB were prepared in the given buffers and incubated for 10 min, and production of yellow color was monitored. pH 7 (HEPES) was chosen as the optimum pH for the coupled assay, both in terms of being optimum for enzyme activity and for DTNB stability.

#### Hexokinase kinetic studies

A G6PDH-coupled assay<sup>30</sup> was used for monitoring the specific activity of hexokinase, as well as for comparing the kinetic properties of ATP $\beta$ S and the native substrate, ATP. For activity measurements, the incubation mixture contained the following: 10 mM glucose, 10 mM  $\text{MgCl}_2$ , 12 mM  $\text{NADP}^+$ , 11 U/mg G6PDH, 100 mM Tris-HCl (pH 8.4) buffer, and 2.5 mM ATP, at 25 °C. The reaction was initiated by addition of hexokinase, and production of NADPH was followed at 340 nm. For steady-state kinetic studies in which ATP was varied, the reaction mixture contained the following: 10 mM  $\text{MgCl}_2$ , 12 mM  $\text{NADP}^+$ , 11 U/mg G6PDH, 10 mM glucose, and 100 mM HEPES, and the ATP concentration was varied from 1 to 20  $\mu\text{M}$ . Reaction was initiated by the addition of 50 U of hexokinase.

The incubation mixture for the DTNB-coupled assay using ATP $\beta$ S (in which ATP $\beta$ S was varied) contained the following: 10 mM  $\text{MgCl}_2$ , 10 mM DTNB, 10 mM glucose, and 100 mM HEPES (pH 7.0), and the ATP $\beta$ S concentration was varied from 1 to 20  $\mu\text{M}$ . The reaction was initiated by the addition of 50 U of hexokinase. The incubation mixture for the DTNB-coupled assay (in which hexokinase concentration was varied) was as above, but with 0.20 mM ATP $\beta$ S. Reactions were initiated by the addition of 3 to 35 U of hexokinase. These reactions were with the preferred ATP $\beta$ S diastereomer (R), but control measurements were also made with the S diastereomer using the same reaction conditions. Inhibition studies were done with varied ADP.

#### Calcium-activated myosin ATPase kinetic studies<sup>31-33</sup>

A PK/LDH-coupled assay was used for monitoring the specific activity of myosin, as well as for comparing the kinetic properties of the native substrate ATP, with ATP $\beta$ S. For activity measurements with ATP, the incubation mixture contained the following: 20  $\mu\text{M}$  NADH, 25 mM phosphoenolpyruvate, 10 U/mL LDH, 50 U/mL PK, 5 mM calcium, 10 mM  $\text{MgCl}_2$ , and 1 mM ATP. The reaction was initiated by the addition of myosin. For kinetic studies in which the ATP was varied, the reaction mixture was as above, but with 4 to 409  $\mu\text{M}$   $\text{Mg}^{2+}$  and 3 to 408  $\mu\text{M}$  ATP. The reaction was initiated by the addition of 10 U of myosin.

The incubation mixture for the DTNB-coupled assay, in which ATP $\beta$ S was varied, contained the following: 10 mM DTNB, 10 U/mL myosin, and 5 mM calcium. The  $\text{Mg}^{2+}$  concentration was kept 1 mM above the ATP $\beta$ S concentration. ATP $\beta$ S was varied from 3.4 to 408  $\mu\text{M}$ , and reactions were initiated by the addition of myosin. The incubation mixture for the DTNB-coupled assay, in which calcium-activated myosin was varied, contained the following: 10 mM DTNB, 32  $\mu\text{M}$  ATP $\beta$ S, and 5 mM calcium. The myosin concentration was varied from 3.4 to 408  $\mu\text{M}$ , and reaction was initiated by the addition of myosin. These reactions were with the preferred ATP $\beta$ S diastereomer (S), but control measurements were also made with the R diastereomer, using the same reaction conditions.

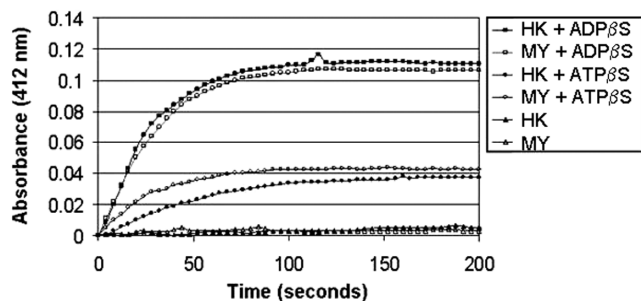


**FIG. 2.** Relative rates of DTNB cleavage by ADP $\beta$ S, ATP $\beta$ S, and protein. Curves designated HK and MY refer to hexokinase- or calcium-activated myosin ATPase assay conditions, respectively. The observed signal for ATP $\beta$ S is due to the presence of the ADP $\beta$ S contaminant in the ATP $\beta$ S sample. The above results demonstrate the selectivity of DTNB toward ADP $\beta$ S relative to ATP $\beta$ S.

**Additional control experiments**

Calcium-activated myosin and hexokinase control assays were performed so as to gain insights into the relative reactivity of ADP $\beta$ S, ATP $\beta$ S, and protein thiols toward DTNB and hence their contributions, if any, to the observed UV absorption signal at 412 nm. The assay mixtures had the same composition as described above, except that only 1 of either ADP $\beta$ S, ATP $\beta$ S, or protein was present. The total assay time was no more than 10 min (**Fig. 2**).

**Fluorescence-coupled assay in plates**

Production of ADP $\beta$ S was also monitored using a fluorescence-based version of the dithio-coupled assay. In place of DTNB, a fluorescent dithio reagent was used (DSSA: **3**), which contained cystine labeled on its amino groups using fluorescein isothiocyanide and rhodamine sulphonyl chloride.<sup>29</sup> The hexokinase assay mixture contained 10 mM MgCl<sub>2</sub>, 10 mM glucose, 10  $\mu$ M DSSA (**3**), 100 mM (pH 7.0) HEPES buffer, and 1 to 5 U/ $\mu$ L hexokinase activity, and ATP $\beta$ S varied from 10 to 120  $\mu$ M. Control reactions used for *Z'* measurements were the same but did not have hexokinase present. Fluorescence measurements were made using a BMG Polarstar fluorimeter equipped with a 96-well plate reader. Excitation was with 10 flashes per measurement, 0.1-sec position delay, and 5 mixing cycles before protein injection to initiate the assay. Initial velocities were measured as fluorescence increased but after a brief decrease in fluorescence, before the steady-state was reached.

**RESULTS AND DISCUSSION**

All kinases and ATPases produce ADP, so an assay that detects ADP would be a universal assay of potential use in enzymology as well as high-throughput screening. To this end, we

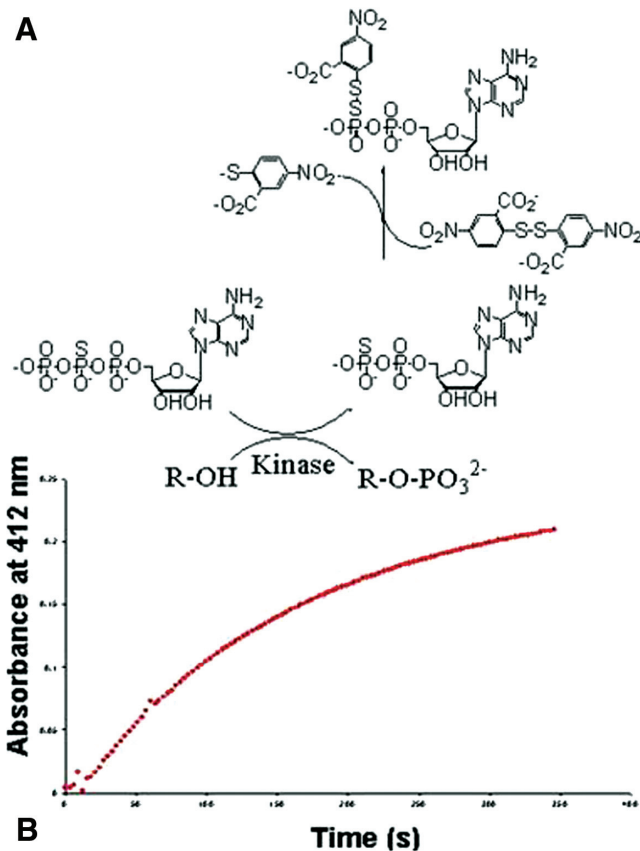


**FIG. 3.** (A) The dithio-coupled kinase assay, using DTNB. (B) A typical progress curve for the DTNB-coupled assay of the myosin ATPase reaction with ATP $\beta$ S. The initial rate is the slope of the steepest part, near the start of the curve.

have developed a chemically coupled assay where ATP $\beta$ S is used as a substrate in place of ATP, and the ADP $\beta$ S that is produced is selectively detected. Such detection is possible because ADP $\beta$ S reacts with dithio groups (**Fig. 3A**), whereas ATP $\beta$ S does not. Therefore, reaction can be followed using dithio reagents such as DTNB (**1**), for a chromogenic assay, or a fluorescent dithio reagent such as DSSA (**3**), for a fluorogenic assay. It is important to note that the dithio reagent is not likely to oxidize the protein significantly in the timeframe of the assay, relative to the reaction being monitored. This is because the protein being assayed is typically present in the low nanomolar range, whereas the ADP $\beta$ S is being produced at concentrations that are several orders of magnitude higher—and conditions are always adjusted such that reaction between ADP $\beta$ S and dithio is at a measurable rate in the timeframe of the assay.

The primary reagent required for the dithio-coupled assay is ATP $\beta$ S, which is not commercially available. But both diastereomers of ATP $\beta$ S (S and R) can be synthesized enzymatically by established methods.<sup>27</sup> <sup>31</sup>P NMR chemical shifts for the enzymatically synthesized ATP $\beta$ S products are in agreement with the

previously reported values<sup>34</sup> of  $-11.4$  ppm (doublet),  $-5.8$  ppm (doublet), and  $30$  ppm (triplet) for the  $\alpha$ ,  $\gamma$ , and  $\beta$  phosphorus atoms, respectively (Fig. 1). Purification of the enzymatically synthesized ATP $\beta$ S on a DEAE column shows reasonable separation from ADP $\beta$ S, which is important because contaminating ADP $\beta$ S would lead to a high background reduction of the dithio probe and may also act as a product inhibitor in the assay. The former is demonstrated in Figure 2, where it can be seen that if residual ADP $\beta$ S is present, there is a burst in signal for both the hexokinase and the myosin assays. If contaminating ADP $\beta$ S is present, both problems can be minimized by first consuming the ADP $\beta$ S by preincubating the reaction mixture before adding kinase. There is little background rate in the absence of ATP $\beta$ S or after residual ADP $\beta$ S is consumed (Fig. 2). Residual ADP $\beta$ S can also be removed by passing over a thiol affinity resin, such as Activated Thiol Sepharose 4B (GE Healthcare, Chalfont St. Giles, UK). But ADP $\beta$ S and other contaminants can usually be avoided at the outset by taking more conservative cuts of fractions during purification (Fig. 1C) and by avoiding prolonged sample concentration via rotary evaporation.

It should be noted that the polyphosphate/phosphorothioate of both ATP $\beta$ S and ADP $\beta$ S are quite stable at high pH, showing no detectable changes in  $^{31}\text{P}$  NMR spectra after 3 weeks at pH 11 (carbonate buffer). Furthermore, ADP $\beta$ S shows only 3% hydrolysis after 3 days at pH 7.4 (HEPES) but nearly complete hydrolysis at pH 3.4 (glycine) in  $< 1$  h. All stability studies were at  $4^\circ\text{C}$  and based on changes in  $^{31}\text{P}$  NMR spectra, so they reflect only the stability of the polyphosphate/phosphorothioate. In terms of stability issues during ATP $\beta$ S preparation, concentration of the enzymatic synthesis reaction mixture using a rotary evaporator often led to some decomposition of ATP $\beta$ S, so lyophilization is preferred. A potential problem is that the enzymatic syntheses have previously been reported to be less than 100% diastereoselective, leading to minor contamination with the undesired diastereomer.<sup>35</sup> But this was not apparent from the  $^{31}\text{P}$  NMR spectra (Fig. 1), perhaps because solutions were too dilute, such that only the major diastereomer ( $> 80\%$ ) could be detected. In any case, diastereotopic purity may not be required for routine assays.

The dithio-coupled assay can be implemented for any kinase or ATPase, simply by substituting ATP with ATP $\beta$ S and adding a dithio coupling reagent such as DTNB or the DSSA probe (Fig. 3A). Although kinases and ATPases will prefer either the R or S diastereomer of ATP $\beta$ S, a mixture of diastereomers can be used, and only 1 will be used by the enzyme. Otherwise, it will be necessary to try both diastereomers to determine the preference for the kinase being studied. Steady-state kinetic rates for the kinase or ATPase reaction are measured from progress curves, monitoring changes in absorbance for DTNB (Fig. 3B) or fluorescence for the DSSA probe (see below). Initial velocities are extracted from the early part of the progress curves. As in any coupled assay, it is important to

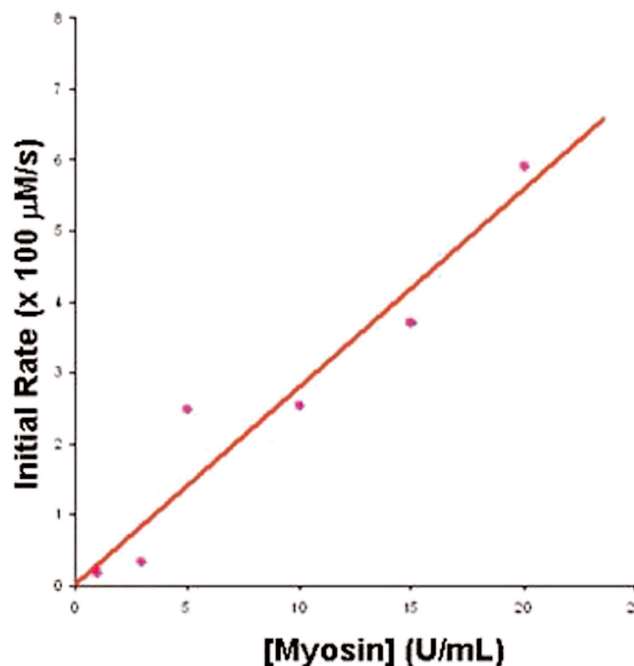


FIG. 4. Validation curve for the myosin ATPase reaction with ATP $\beta$ S (S diastereomer), using the DTNB-coupled assay. Each point is an initial rate from a progress curve, such as in Figure 3.

make sure that the reaction rate is proportional to enzyme concentration and not limited by rate of reaction in the coupling step (ADP $\beta$ S reaction with DTNB). This was demonstrated with a validation curve for the myosin ATPase reaction (Fig. 4). Once an enzyme concentration is chosen from the linear part of the validation curve, a full steady-state kinetic analysis can be performed, as shown in Figure 5B for calcium-activated myosin ATPase. Therefore, steady-state kinetic analyses can be pursued using the dithio-coupled assay (Fig. 5B) as an alternative to the widely used PK/LDH-coupled assay (Fig. 5A). Thorough steady-state analysis is required to establish the mechanism of inhibition (as competitive, noncompetitive, or uncompetitive) for inhibitors identified from screening campaigns. The preference of myosin for the S diastereomer of ATP $\beta$ S<sup>27</sup> could be clearly demonstrated, although this could also be done more simply in a higher throughput screen by simply comparing progress curves for ATP $\beta$ S (R) and ATP $\beta$ S (S) diastereomers.

Interestingly, the validation curve for the DTNB-coupled assay with hexokinase indicates that at higher concentrations, the reaction rate is no longer proportional to enzyme concentration (Fig. 6). This emphasizes the importance of doing validation curves to choose an appropriate enzyme concentration, as is routine practice for any coupled assay. At an appropriate lower enzyme concentration, the DTNB-coupled assay could be used for a steady-state analysis of hexokinase as well (Fig. 7). In this

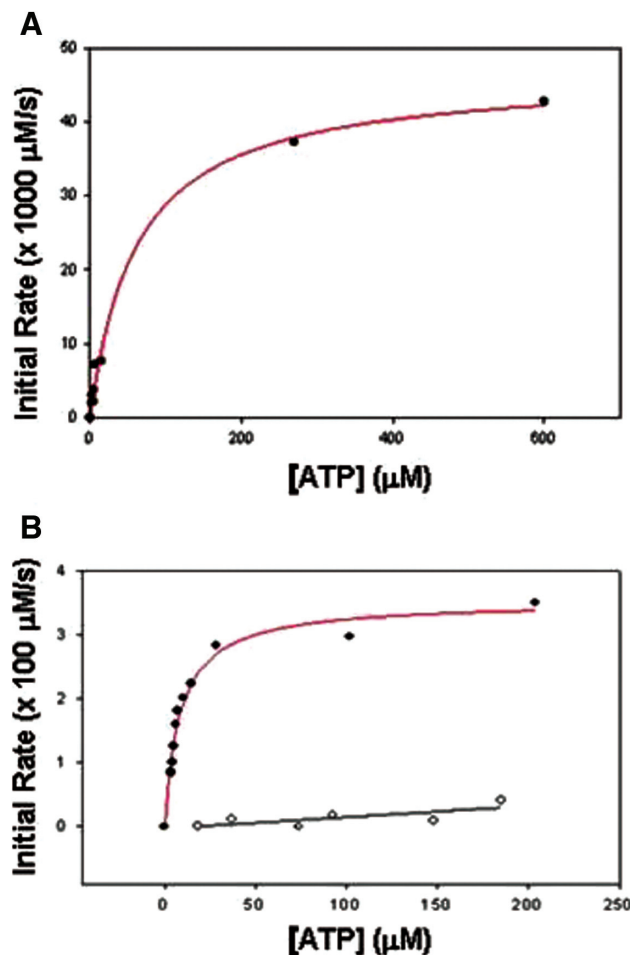


FIG. 5. (A) Initial velocity plot, showing Michaelis-Menton kinetics with respect to adenosine triphosphate (ATP) concentration for the myosin ATPase reaction. Initial velocities were measured with the pyruvate kinase (PK)/lactate dehydrogenase (LDH)-coupled assay. (B) Initial velocity plot, showing Michaelis-Menton kinetics with respect to ATPβS concentration for the myosin ATPase reaction. Initial velocities were measured with the DTNB-coupled assay. Assay was performed with the S diastereomer (filled circles) or R diastereomer (open circles) of ATPβS.

case, the preference of hexokinase for the R diastereomer of ATPβS could also be clearly demonstrated.

For both hexokinase and myosin, there was a modest decrease in  $K_m$  for ATPβS relative to ATP (Table 1). This is actually an advantage in the assay because it means that less ATPβS is required, with the optimal cofactor concentration in the assay determined relative to its  $K_m$ . This reduced  $K_m$  value would have no effect on the measured  $K_i$  (or  $IC_{50}$ ) for a kinase inhibitor because  $K_i$  is not a function of  $K_m$  for ATPβS but rather of the [cofactor]/ $K_m$  ratio chosen for the assay. Also, it should be noted

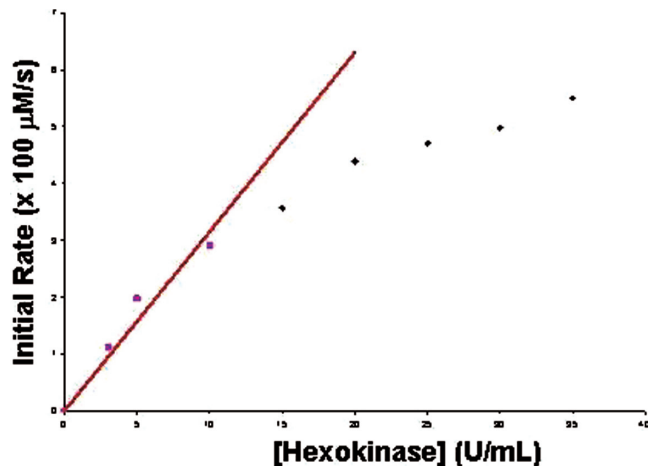


FIG. 6. Validation curve for the hexokinase reaction with ATPβS (R diastereomer), using the DTNB-coupled assay.

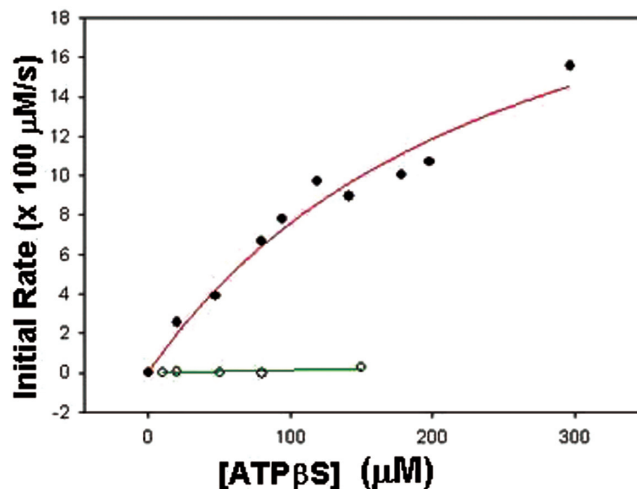


FIG. 7. Initial velocity plot, showing Michaelis-Menton kinetics with respect to ATPβS concentration, for the hexokinase reaction. Initial velocities were measured with the DTNB-coupled assay. Assay was performed with the R diastereomer (filled circles) or S diastereomer (open circles) of ATPβS.

that this assay will detect any kinase inhibitor, irrespective of whether it binds in the ATP site, because it monitors inhibition of the reaction rate, not simply competitive displacement.

Sensitivity of the assay is greater than that of NADH-coupled assays due to the higher extinction coefficient of DTNB. As such, it should be possible to detect ADPβS concentrations as low as 0.1 μM and as high as 100 μM in a 1-cm path-length cuvette. One should therefore adjust enzyme concentration so that the first 5% to 10% of the reaction is being read in the desired timeframe (e.g., 10-60 min) within this

**Table 1. Effect of the O to S Substitution on Michaelis Constants**

Enzyme	Nucleotide	$K_m$ ( $\mu\text{M}$ )	$K_m^a$
Myosin	ATP $\beta$ S (S)	15 $\pm$ 1	0.35
	ATP	42 $\pm$ 10	1.00
Hexokinase	ATP $\beta$ S (R)	3.7 $\pm$ 0.6	0.06
	ATP	61 $\pm$ 1	1.00

ATP, adenosine triphosphate.

a. Relative  $K_m$ .

dynamic range. Unlike assays that detect decreasing fluorescent or visible signal (e.g., NADH-coupled assays), one can increase the detectable probe's concentration in order to push the equilibrium for the reaction—to produce more linear progress curves. Further sensitivity can be achieved with fluorescent thiol detection probes (see below).

A potential concern with this assay is that the dithio probe may be reduced by added protein reductants, such as DTT (dithiothreitol), TCEP (Tris(2-carboxyethyl)phosphine), or  $\beta$ -ME ( $\beta$ -mercaptoethanol). For proteins that require thiol reductants for activity, especially when detecting with DTNB (DSSA does not easily oxidize proteins), it is best to maintain the enzyme stock solution in 1 mM  $\beta$ -ME, then to dilute it into an assay mixture that has no reductant (a 1:40 dilution would produce only 25  $\mu\text{M}$   $\beta$ -ME in the assay). For the brief period of the assay, there is usually little oxidation of protein thiols. This approach has been taken in an inhibition assay with hexokinase (Fig. 8), where a hexokinase stock was maintained in 1 mM  $\beta$ -ME and then diluted into an assay mixture that had no thiol reductant. Hexokinase has 5 cysteines and no disulfide bonds. The  $\text{IC}_{50}$  obtained for the ADP inhibitor of hexokinase was the same with  $\beta$ -ME present ( $\text{Log}(\text{IC}_{50}) = 2.8 \pm 0.3$ ) as it was without  $\beta$ -ME present ( $\text{Log}(\text{IC}_{50}) = 3.0 \pm 0.3$ ), and it was in reasonable agreement with the previously reported  $\text{Log}(K_i)$  of 3.2.<sup>36</sup> The concern over protein oxidation by thiol detection probe is lessened if DSSA is used due to its low reduction potential ( $E^{\circ'} = 0.6 \text{ V}$ ).<sup>29</sup> The DSSA probe is also not easily reduced by protein thiol reductants such as  $\beta$ -ME. Of the commonly used protein reductants,  $\beta$ -ME reacts the slowest with the fluorescent probe (Fig. 9), so it is the preferred reagent to use.

Because this dithio-coupled assay may be useful for the HTS of kinases and ATPases, a fluorescent version of the assay using the DSSA probe is being developed as well. As just discussed, this version of the assay is advantageous because DSSA is less likely to cause any oxidation of protein thiols (and has decreased reactivity with  $\beta$ -ME). The fluorescent form of the assay is similar to that described above, but DTNB is replaced with a fluorescent dithio probe such as DSSA (3). The fluorescent probe is reduced by ADP $\beta$ S in the same manner as DTNB, but it can be present at a much lower concentration. It

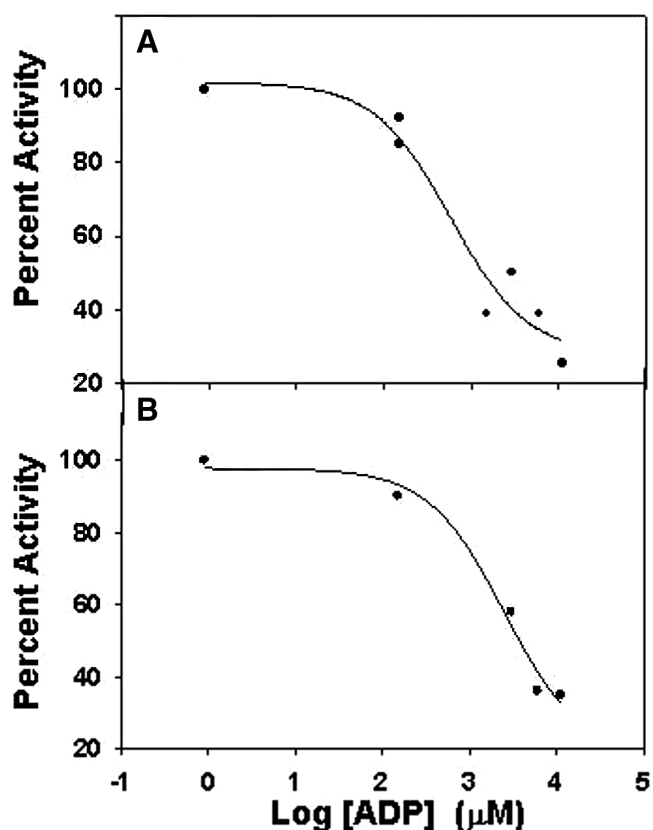


**FIG. 8.** Effects of  $\beta$ -mercaptoethanol ( $\beta$ -ME) on  $\text{IC}_{50}$  measurements. (A) Dose-response curve for inhibition of hexokinase by adenosine diphosphate (ADP), using a hexokinase stock solution that had 1 mM  $\beta$ -ME protein reductant present but was then diluted 1:40 into the final assay. Fitted  $\text{Log}(\text{IC}_{50})$  was  $2.8 \pm 0.3$ . (B) The same assay, but performed using a hexokinase stock solution that had no reductant present, gave fitted  $\text{Log}(\text{IC}_{50})$  values of  $2.6 \pm 0.4$  and  $3.4 \pm 0.2$  in 2 separate experiments, for an average  $\text{Log}(\text{IC}_{50})$  of 3.0. The assay mixture contained 2 mM DTNB, 10 mM glucose, 10 mM  $\text{MgCl}_2$ , 10 U/mL hexokinase, 0.1 mM ATP $\beta$ S, and 100 mM HEPES (pH 7.0). Assay was initiated with substrate (glucose and  $\text{Mg}^{2+}$ ), after initial consumption of any residual thiols.

is typically present at a 1- to 10- $\mu\text{M}$  concentration, whereas ADP $\beta$ S is present in a much larger excess. Because of the low redox potential of the DSSA probe ( $E^{\circ'} = -0.60 \text{ V}$ ),<sup>29</sup> significant reduction is observed only at high concentrations of thiol, and the rate of fluorescence change remains linearly dependant on thiol concentration.

The fluorescence assay was validated in a 96-well plate format by comparing initial velocities in the presence or absence of hexokinase and in triplicate, so that  $Z'$  values<sup>37</sup> could be calculated according to the following equation:

$$Z' = 1 - \frac{3 \cdot \text{SD}(\text{hexokinase}) + 3 \cdot \text{SD}(\text{blank})}{\text{Vo}(\text{hexokinase}) - \text{Vo}(\text{blank})}$$

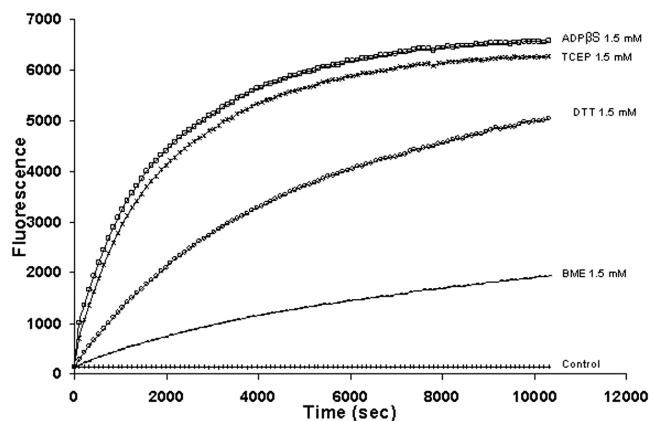


**FIG. 9.** Relative reactivity of ADPβS and various protein reductants (present at 1.5 mM) with the DSSA thiol detection probe (3) present at 5 μM in a 100-mM Tris buffer, pH 8.2.

The assay was performed at ATPβS concentrations of 10, 20, 30, 40, 60, 90, and 120 μM (Fig. 10), and the average Z' value was 0.54.

### CONCLUSIONS

The general kinase and ATPase assay presented herein is a simple, reliable, and sensitive way of measuring enzyme activity, using ATPβS as substrate. It was demonstrated that ADPβS reacts very rapidly with DTNB compared to ATPβS and protein, the other sources of free thiols in the assay. Although the dithio-coupled assay needs to be tested on other kinases, it should be a universal assay because it relies on detection of ADPβS, a broadly tolerated analogue of ADP, the product common to all kinase and ATPase reactions. The results from the chromogenic assay using DTNB have clearly shown that for hexokinase and myosin, this assay is effective. If desired, the diastereoselectivity of an enzyme toward the ATPβS diastereomers can also be determined to classify kinase active sites. Finally, a fluorescence version of this assay is robust enough for HTS of kinases because the Z' value of 0.54 is above the recommended value of 0.5 for HTS assays.

### ACKNOWLEDGMENT

This work was supported in part by grants from the American Heart Association (AHA-0530307Z) to D.S.S. and from the Department of Defense (W81XWH-05-1-0476) to P.K.P.

### REFERENCES

1. Knighton DR, Zheng JH, Ten Eyck LF, Ashford VA, Xuong NH, Taylor SS, et al: Crystal structure of the catalytic subunit of cyclic adenosine monophosphate-dependent protein kinase. *Science* 1991;253:407-414.

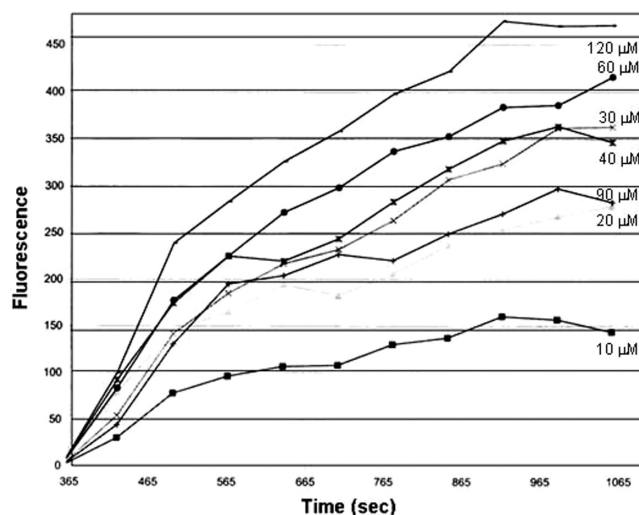


**FIG. 10.** Progress curves for the hexokinase reaction using ATPβS (R diastereomer) and the DSSA-coupled fluorescence assay (excitation = 485 nm; emission = 520 nm). Detection was in 96-well plates using a BMG Polarstar plate reader. ATPβS concentrations were varied, as indicated by each curve.

2. Manning G, Whyte DB, Martinez R, Hunter T, Sudarsanam S: The protein kinase complement of the human genome. *Science* 2002;298:1912-1934.
3. Cohen P: The role of protein phosphorylation in human health and disease. The Sir Hans Krebs Medal Lecture. *Eur J Biochem* 2001;268:5001-5010.
4. Valigra L: Varying approaches to inhibiting kinase. *Drug Disc Develop* 2005;8:51-55.
5. Parker GJ, Law TL, Lenoach FJ, Bolger RE: Development of high throughput screening assays using fluorescence polarization: nuclear receptor-ligand-binding and kinase/phosphatase assays. *J Biomol Screen* 2000;5:77-88.
6. Prokopowicz AS, Brown MP, Wildeson JM, Jakes S, Labadia ME: Fluorescent probes for use in protein kinase inhibitor binding competition assays for screening applications. *PCT Int Appl* 2005;49.
7. Shults MD, Imperiali B: Versatile fluorescence probes of protein kinase activity. *J Am Chem Soc* 2003;125:14248-14249.
8. Armstrong C, Cohen P: Assaying protein kinase activity using a common seven-residue epitope substrate and phospho-specific antibodies. *PCT Int Appl* 2003;48.
9. Ruzzene M, Pinna LA: Assay of protein kinases and phosphatases using specific peptide substrates. In Hardie G (ed): *Protein Phosphorylation: A Practical Approach*. 2nd ed. Oxford, UK: Oxford University Press, 1999.
10. Umezawa Y: Assay and screening methods for bioactive substances based on cellular signaling pathways. *Rev Mol Biotechnol* 2002;82:357-370.
11. Singh P, Lillywhite B, Bannaghan C, Broad P: Using IMAP technology to identify kinase inhibitors: comparison with a substrate depletion approach and analysis of the nature of false positives. *Comb Chem High Throughput Screen* 2005;8:319-325.
12. Turek-Etienne TC, Kober TP, Stafford JM, Bryant RW: Development of a fluorescence polarization AKT serine/threonine kinase assay using an immobilized metal ion affinity-based technology. *Assay Drug Develop Technol* 2003;1:545-553.
13. Singh P, Harden BJ, Lillywhite BJ, Broad PM: Identification of kinase inhibitors by an ATP depletion method. *Assay Drug Develop Technol* 2004;2:161-169.

14. Koresawa M, Okabe T: High-throughput screening with quantitation of ATP consumption: a universal non-radioisotope, homogeneous assay for protein kinase. *Assay Drug Develop Technol* 2004;2:153-160.
15. Badalassi F, Nguyen HK, Crotti P, Reymond J-L: A selective HIV-protease assay based on a chromogenic amino acid. *Helv Chim Acta* 2002;85:3090-3098.
16. Klein G, Reymond JL: An enantioselective fluorometric assay for alcohol dehydrogenases using albumin catalysed  $\beta$ -elimination of umbelliferone. *Bioorg Med Chem Lett* 1998;8:1113-1116.
17. Wahler D, Reymond J-L: The adrenalin test of enzymes. *Angew Chem Intl Ed Engl* 2002;41:1229-1232.
18. Klein G, Reymond JL: An enantioselective fluorogenic assay of acetate hydrolysis for detecting lipase activity antibodies. *Helv Chim Acta* 1999;3:400-408.
19. Sevestre A, Helaine V, Guyot G, Martin C, Hecquet L: A fluorogenic assay for trans ketolase from *S. cerevisiae*. *Tetrahedron Lett* 2003;44:827-830.
20. Gao W, Xing B, Tsein RY, Rao J: Novel fluorogenic substrates for imaging  $\beta$ -lactamase gene expression. *J Am Chem Soc* 2003;125:11146-11147.
21. Gutierrez MC, Slegers A, Simpson HD, Alphand V, Furstoss R: The first fluorogenic assay for detecting a Baeyer-villagerase activity in microbial cells. *Org Biol Chem* 2003;1:3500-3506.
22. Veldhuyzen WF, Nguyen Q, McMaster G, Lawrence DS: A light activated probe for intracellular protein kinase activity. *J Am Chem Soc* 2003;125:13358-13359.
23. Simeonov A, Bi X, Nikiforov TT: Enzyme assays by fluorescence polarization in the presence of polyarginine: study of kinase, phosphatase and protease reactions. *Anal Biochem* 2002;304:193-199.
24. Kupcho K, Somberg R, Bulleit B, Goueli SA: A homogeneous non radioactive high throughput fluorogenic protein kinase assay. *Anal Biochem* 2003;317:210-217.
25. Martin K, Steinberg TH, Cooley LA, Gee KR, Beechem JM, Patton WF: Quantitative analysis of protein phosphorylation status and kinase activity in microarrays using a novel protein phosphorylation sensor dye. *Proteomics* 2003;3:1244-1255.
26. Ojida A, Mitooka Y, Inoue M, Hamachi I: First artificial receptors and chemosensors toward phosphorylated peptides in aqueous solution. *J Am Chem Soc* 2002;124:6256-6258.
27. Eckstein F, Goody RS: Synthesis and properties of diastereomers of adenosine 5'-(O-1-thiotriphosphate) adenosine 5'-(O-2-thiotriphosphate). *Biochemistry* 1976;15:1685-1691.
28. Silverstein RM: The determination of the molar extinction coefficient of reduced DTNB. *Anal Biochem* 1975;63:281-282.
29. Pallela PK, Chiku T, Carvan MJ, Sem DS: Fluorescence-based detection of thiols *in vitro* and *in vivo* using dithiol probes. *Anal Biochem* 2006;352:265-273.
30. Wilson K, Walker J: *Principles and Techniques of Practical Biochemistry*. 5th ed. Cambridge, UK: University of Cambridge Press, 2000.
31. Pollard TD: Assays for myosin. *Methods Enzymol (Part B)* 1982;85:123-130.
32. Chacko S, Conti MA, Aldestein RS: Effect of phosphorylation of smooth muscle myosin on actin activation and calcium ion regulation. *Proc Natl Acad Sci USA* 1977;74:129-133.
33. Morris CA, Wells AL, Yang Z, Chen L, Baldacchiono CV, Sweeney HL: Calcium functionally uncouples the heads of myosin VI. *J Biol Chem* 2003;278:23324-23330.
34. Jaffe EK, Cohn M: Phosphorous-31 nuclear magnetic resonances of the thiophosphate analogues of adenine nucleotides: effects of pH and  $Mg^{2+}$  binding. *Biochemistry* 1978;17:652-657.
35. Jaffe EK, Cohn M: Diastereomers of the nucleoside phosphothioates as probes of the structure of the metal nucleotide substrates and of the nucleotide binding site of yeast hexokinase. *J Biol Chem* 1979;254:10839-10845.
36. Viola RE, Raushel FM, Rendina AR, Cleland WW: Substrate synergism and the kinetic mechanism of yeast hexokinase. *Biochemistry* 1982;21:1295-1302.
37. Zhang ZH, Chung TDY, Oldenburg KR: A simple statistical parameter for use in evaluation and validation of high throughput screening assays. *J Biomol Screen* 1999;4:67-73.

Address reprint requests to:

Daniel S. Sem  
Chemical Proteomics Facility at Marquette  
Department of Chemistry  
Marquette University, P.O. Box 1881  
Milwaukee, WI 53201-1881

E-mail: Daniel.Sem@mu.edu